Stratospheric Flow during Two Recent Winters Simulated by a Mechanistic Model

PHILIP W. MOTE,* PETER A. STOTT,+ AND ROBERT S. HARWOOD

Department of Meteorology, University of Edinburgh, Edinburgh, United Kingdom

(Manuscript received 3 September 1996, in final form 25 June 1997)

ABSTRACT

The authors have used a spectral, primitive equation mechanistic model of the stratosphere and mesosphere to simulate observed stratospheric flow through the winters of 1991–92 and 1994–95 by forcing the model at 100 hPa with observed geopotential height. The authors assess the model's performance quantitatively by comparing the simulations with the United Kingdom Meteorological Office (UKMO) assimilated stratosphere–troposphere data. Time-mean, zonal-mean temperatures are generally within 5 K and winds within 5 m s^{-1}; transient features, such as wave growth, are mostly simulated well. The phase accuracy of planetary-scale waves declines with altitude and wavenumber, and the model has difficulty correctly simulating traveling anticyclones in the upper stratosphere. The authors examine the minor warming of January 1995 which was unusual in its depth and development and which the model simulated fairly well. The authors also examine the minor warming of January 1992, which the model missed, and a major warming in February 1992 that occurred in the model but not in the observations.

1. Introduction

Because the troposphere exerts considerable influence on the stratosphere through dynamical and radiative means, the stratosphere might intuitively seem to be entirely subject to the troposphere, responding linearly, or at least directly, to forcing from below. Indeed, upward propagation of waves of various scales from the troposphere to the stratosphere explains a whole range of dynamical phenomena in the stratosphere, from the slowly varying quasi-biennial oscillation (QBO) in the Tropics to the rapid changes during a sudden polar warming. Yet the ways in which the troposphere influences the stratosphere are myriad and complex.

Mechanistic models of the stratosphere and mesosphere have long been used to identify which aspects of tropospheric forcing are important to the dynamics of the stratosphere. Such models have been used extensively to study stratospheric sudden polar warmings (e.g., Matsuno 1971), especially the February 1979 sudden warming (Butchart et al. 1982; Smith 1992; Manney et al. 1994; Kouker et al. 1995). Mechanistic models have also been used to study the QBO (e.g., O'Sullivan and Young 1992), inertial instability (O'Sullivan and Hitchman 1992), and the effect of planetary waves on the distribution of ozone (Ushimaru and Tanaka 1994). Mechanistic models have also been used to study seasonal evolution of stratospheric flow and to isolate relevant aspects of the tropospheric forcing. Two examples are the simulation of southern winter by Fisher et al. (1993) and Farrara et al. (1992); Farrara et al. (1992) used both full and simplified (e.g., wave 1 only) lower boundary and initial conditions.

In this paper we use a new mechanistic model to study stratospheric flow during two northern winters, 1991–92 and 1994–95. Our purposes are 1) to analyze the observed flow during these two winters, augmenting previous studies, and 2) to evaluate the model's performance at simulating time-mean and transient features of the observed flow. Whereas previous studies with mechanistic models have generally focused on events or phenomena, we aim to compare general features of the flow, though we do focus on the minor warmings of January 1992 and January 1995. Another difference from previous studies is that most of them compared model output with NMC (National Meteorological Center, now known as the National Centers for Environmental Prediction—NCEP) analyses in which winds are derived from geopotential height data using a balance equation, whereas we make use of the United Kingdom Meteorological Office (UKMO) assimilated data; the advantages will be enumerated below. Also, our model includes a more elaborate treatment of gravity wave drag, unlike most studies which use simple linear relaxation (Rayleigh friction).

* Current affiliation: NorthWest Research Associates, Bellevue, Washington.

+ Current affiliation: Hadley Centre for Climate Prediction and Research, Meteorological Office, Bracknell, United Kingdom.

Corresponding author address: Dr. Philip W. Mote, NorthWest Research Associates, Inc., P.O. Box 3027, Bellevue, WA 98009.
E-mail: mote@nwra.com

In section 2 we describe the model and in section 3 the UKMO data. Section 4 defines the diagnostics used. Sections 5 and 6 each focus on one winter, comparing the model runs with observations. In section 7 we discuss sudden warmings during the two observed and simulated winters.

2. The model

The three-dimensional, primitive equation mechanistic model used in this paper, the USMM (for UGAMP Stratosphere–Mesosphere Model), is a spectral model, unlike the commonly used UKMO mechanistic model (e.g., Fisher et al. 1993). The USMM traces its origins to the 1987 European Centre for Medium-Range Weather Forecasts (ECMWF) forecast model. The ECMWF forecast model was first adapted for climate studies to become the UGAMP (United Kingdom Universities' Global Atmospheric Modeling Programme) GCM, or UGCM, then extended into the upper stratosphere and mesosphere to become the EUGCM, a task that required improving the treatment of radiation and of gravity wave drag (Thuburn 1992).

To make the EUGCM into the mechanistic model, several changes are required.[1] First, all physical processes except radiation and gravity wave drag are turned off. Second, vertical velocities at the lower boundary are calculated by vertically integrating the divergence, and vertical advection of momentum and heat is accomplished by assuming that the winds and temperature in the half-level below the lower boundary are the same as those in the lowest level. The third major change involves the radiation. Like the EUGCM, the USMM uses the MIDRAD radiation scheme (Thuburn and Shine 1991), but in the USMM, since infrared emissions are not calculated in the troposphere, upward fluxes of infrared radiation must be specified at the lower boundary. These fluxes are specified in the 15-μm (CO_2) and 9.6-μm (O_3) bands. W. Lahoz (University of Reading) has used MIDRAD to calculate seasonally and meridionally varying fluxes in these bands at 100 hPa by assuming that emission at 9.6 μm originates at 700 hPa and emission at 15 μm originates at 130 hPa. Temperatures at these levels are used to calculate infrared emissions, and temperatures at 400 and 115 hPa are also used in the radiative transfer calculation (W. Lahoz 1996, personal communication). The fluxes of infrared radiation calculated in this way produce a much better temperature distribution in the lower stratosphere than did other methods of specifying the radiative fluxes.

Many aspects of the USMM configuration can be specified by the user: the resolution, the time step, the vertical coordinate, the altitude of the lower boundary, and the treatment of subgrid-scale momentum forcing. In these runs we use a horizontal resolution of T42 (about $2.8° \times 2.8°$), a vertical resolution of L34 (about 1.6 km, increasing in the top few levels) at pressures ranging from 89.5 to 0.01 hPa, and a time step of 10 min. Although the uppermost full level of the model is at a pressure of 0.01 hPa, the upper boundary of the USMM is at zero pressure. There is therefore no mass flow through the upper boundary. To diminish the possibility of wave reflection, the model has extra scale-selective dissipation, and the short radiative timescale helps to damp waves in the mesosphere. We force the model at 100 hPa using 6-h ECMWF analyses (interpolated to the present time step). We could instead use daily UKMO analyses, but we used ECMWF analyses in order to facilitate another study, to be presented elsewhere. Subgrid-scale momentum forcing is provided by a nonorographic gravity wave drag scheme. Developed by D. Jackson and extended by J. Thuburn and W. Norton, it is based on the orographic gravity wave drag scheme of Palmer et al. (1986) and is intended to represent the effects of both stationary and nonstationary gravity waves which, in the real world, could be forced by processes such as convection or geostrophic adjustment.

For both winters, the code and model configuration were identical. Initial zonally varying wind and temperature fields on 1 November (1991 and 1994) are taken from the UKMO assimilated data. From the top UKMO level at 0.3 hPa to the top USMM level at 0.01 hPa the winds and temperature are extrapolated using thermal-wind balance in the zonal mean.

3. UKMO assimilated data

As part of the correlative database for the *Upper Atmosphere Research Satellite* (*UARS*) project, the UKMO has been running its assimilation model in a troposphere–stratosphere configuration since October 1991. The assimilation procedure and the data are described in detail by Swinbank and O'Neill (1994). The UKMO general circulation model digests input from radiosondes and satellites (chiefly temperatures measured by the stratospheric sounding unit) while maintaining dynamical balance. It then runs for one day and the result serves as the ''first guess'' for the next round of input. The results are interpolated to the *UARS* vertical grid which has pressure levels separated by a factor of $10^{1/6}$ in pressure; thus, the levels that primarily concern us in this paper are at 100, 68, 46, 32, 22, 15, 10, 6.8, and so on to 0.32 hPa. In most of the plots shown in this paper, USMM output has been interpolated to the *UARS* vertical grid, and where direct comparison is needed, UKMO data have been interpolated to the USMM (T42) horizontal grid.

There are a number of advantages of UKMO data compared to the frequently used NMC data. With UKMO data, the vertical extent is greater (three levels

[1] Some of the following discussion is based on notes by J. Thuburn and R. Brugge (1995, personal communication).

in the mesosphere), the vertical resolution is better, and the winds are calculated by a primitive equation model using some observed winds, whereas NMC winds are calculated from temperatures using a balance equation, an approach that leads to considerable uncertainties in the Tropics.

From the beginning of the UKMO dataset to the present, there have been numerous changes to the assimilation model, though these are not expected to have a large impact in most of the stratosphere (R. Swinbank 1996, personal communication). At the beginning, subgrid-scale wave drag—of great importance to the momentum budget in the upper stratosphere and mesosphere (e.g., Boville 1995)—was neglected. As a consequence, by early December 1991, wind speeds in the developing winter vortex became so large in the upper stratosphere that the assimilation model became numerically unstable and was turned off for a time. When it was restarted, Rayleigh friction was used to reduce the wind speeds at upper levels (Swinbank and O'Neill 1994). The missing days were later filled in.

4. Diagnostic quantities

a. Eliassen–Palm flux

The Eliassen–Palm (EP) flux vector **F** (Edmon et al. 1980) appears when the Eulerian-mean momentum equation is rewritten in transformed-Eulerian mean form (Andrews et al. 1987, 128). To the extent that the WKB approximation holds (e.g., Butchart et al. 1982), the direction and magnitude of **F** indicate the direction and intensity of planetary-scale Rossby wave propagation, and the divergence of **F** indicates where these waves decelerate (or occasionally accelerate) the zonal mean wind $\overline{u}$. Its components in spherical coordinates are $\mathbf{F} = (0, F_\phi, F_z)$, where

$$F_\phi = \rho_0 a \cos\phi \left[\frac{\partial \overline{u}}{\partial z} \frac{\overline{v'T'}}{(\partial T/\partial z + \kappa \overline{T}/H)} - \overline{u'v'} \right] \quad (1)$$

and

$$F_z = \rho_0 a \cos\phi \left\{ \left[f - \frac{1}{a \cos\phi} \frac{\partial}{\partial \phi} (\overline{u} \cos\phi) \right] \frac{\overline{v'T'}}{(\partial \overline{T}/\partial z + \kappa \overline{T}/H)} - \overline{u'\omega'} \frac{H}{p} \right\}. \quad (2)$$

Here ϕ is latitude, $z = -H \log p/p_0$, a is the radius of the earth, and ρ_0 is a mean density profile. These equations are written using u, v, T, p, and ω, quantities that are (with one exception) available from both the UKMO assimilated data and as output from the USMM. The exception is that for 1991–92, ω was not available in the UKMO data and consequently the $\overline{u'\omega'}$ term has been omitted from the calculation in both UKMO and USMM for that winter. This approximation is justifiable since in general the term in $\overline{u'\omega'}$ is much smaller than the other term and in any case we are using a consistent method for UKMO data and USMM output during each winter.

We also examined the refractive index Q_k(Butchart et al. 1982), but did not find it to be a useful way to characterize differences in wave propagation. According to theory, waves should be refracted toward high refractive index, and although they generally were, differences in the refractive index distribution did not correspond to differences in the *direction* of **F** but sometimes did correspond to differences in the magnitude of **F**. Conversely, Randel et al. (1987) found that very similar distributions of refractive index occurred on days when the field of **F** was vastly different. The derivations of **F**, its divergence, and Q_k treat the stratosphere in the zonal mean, and the interpretation of Q_k as an indicator of wave propagation assumes that wave amplitudes are small and that waves vary slowly and interact only weakly. Yet during dynamically active periods when **F** and Q_k are of greatest interest, waves can be large, rapidly varying and strongly interacting. Furthermore, zonal means can hide interesting and important features like the growth and merger of anticyclones (e.g., O'Neill and Pope 1988) and the displacement of the vortex.

b. Vortex displacement vector

Given the potential shortcomings of EP fluxes during interesting periods in the stratosphere, we introduce a diagnostic quantity that focuses on the behavior of the polar vortex as a three-dimensional entity: a vector whose length and orientation indicate, respectively, the colatitude and longitude of the vortex center relative to the pole, where the vortex center is defined as the minimum in the geopotential height field on a pressure surface. This quantity, the ''vortex displacement,'' is purely descriptive and has no dynamical basis, but as we shall see, it offers a useful way of viewing the flow.

When this manuscript was in revision, the authors learned of a new ''elliptical diagnostic'' developed by Waugh (Waugh 1997), in which ellipses are fitted to contours of potential vorticity, thereby allowing the vortex to be characterized not only by area (as is often done) but also by displacement, orientation, and aspect ratio. These diagnostics are well suited to our comparison, but with limited time we did not apply them.

c. PV area

Maps of Ertel's potential vorticity (commonly known as PV) are one way of visualizing the instantaneous flow. Large meridional gradients of PV are well correlated with the chemical boundary of the polar vortex, as defined by long-lived stratospheric tracers like N_2O. A good way to view the evolution of the polar vortex through a season is the PV area diagnostic (Butchart and Remsberg 1986). The area within a PV contour is calculated and expressed as an ''equivalent latitude,''

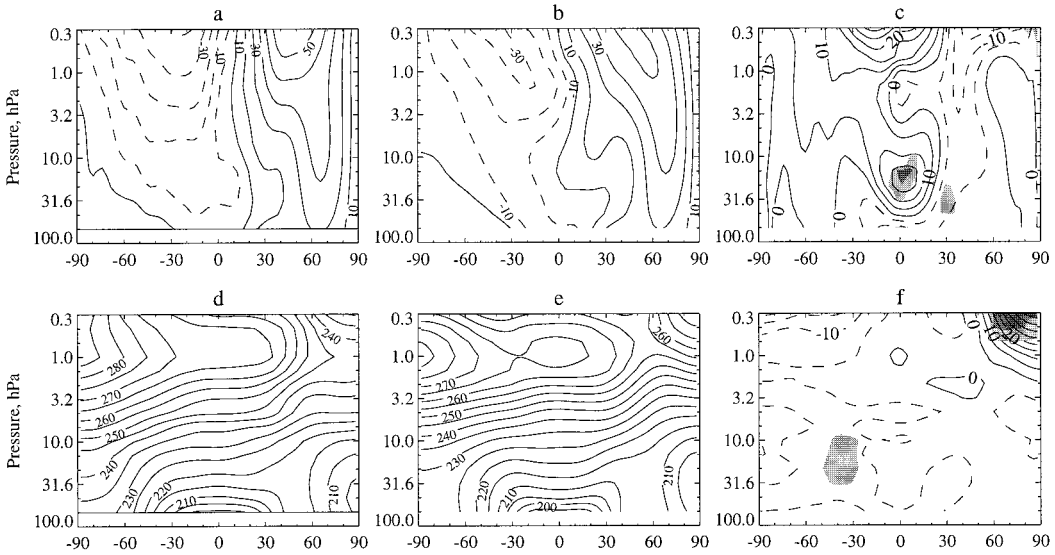

FIG. 1. Zonal mean zonal wind $\overline{u}$ and temperature $\overline{T}$ for November 1991–February 1992. (a) Observed (UKMO) and (b) modeled (USMM) $\overline{u}$; (c) difference in $\overline{u}$, USMM − UKMO. (d) Observed and (e) modeled $\overline{T}$; (f) difference in $\overline{T}$, USMM − UKMO. Statistically significant differences at the 5% and 1% levels are shaded light and dark, respectively.

that is, the latitude enclosing the same area on the sphere.

5. Description of observed and modeled 1991–92 winter

a. Comparison of zonal mean winds and temperatures

Due to the problems with UKMO data (mentioned in section 3) in late November and early December 1991, a comparison of the USMM output with UKMO data is unlikely to be meaningful in the upper stratosphere before early December 1991. Below 1 hPa, however, differences between UKMO and USMM temperatures were generally less than 5 K, and wind differences were less than 5 m s^{-1} except in the Tropics.

Figure 1 shows the time-mean $\overline{u}$ and $\overline{T}$ for November 1991 through February 1992. In the USMM, both the polar night jet and the subtropical easterly jet tilt with height in the upper stratosphere, unlike the jets in the UKMO data. In the Tropics, the phase of the observed quasi-biennial oscillation (QBO) was easterly during this period, but the USMM has a lobe of westerlies centered at about 30 hPa. The difference is part of a pattern, with a westerly bias in the lower mesosphere, easterly in the upper stratosphere, westerly in the middle stratosphere, and easterly in the lower stratosphere. These areas of persistent bias are fairly symmetric about the equator. Note that statistically significant differences are rare. (Statistical significance was calculated using the Student's t-test, where the number of degrees of freedom at each point in the latitude–height plane for each data set was determined by dividing the number of days by the autocorrelation time.) Because the QBO is forced by waves of varying scales (e.g., Andrews et al. 1987), many of which are not resolved in the data used as a lower boundary condition for the USMM, we would not expect a realistic QBO to appear in the USMM. However, general circulation models mostly have an *easterly* bias in the tropical lower stratosphere (e.g., Boville 1995).

The temperature distribution is fairly similar for the UKMO and the USMM, but they differ over the winter stratopause, where the UKMO is persistently colder than the USMM during both winters that we simulated. UKMO temperatures there are lower than NMC temperatures as well (Swinbank and O'Neill 1994; Manney et al. 1996b), perhaps due to the treatment of subgrid-scale wave drag in the UKMO model. In the Southern Hemisphere, the USMM has lower temperatures and weaker easterlies than observed. At northern high latitudes the USMM has slightly stronger westerlies in the time mean. In virtually all of the stratosphere the USMM is slightly colder than the UKMO. Overall, about 50% of points in the latitude–height plane have an absolute temperature difference of less than 5 K.

Figure 2 shows the standard deviations, at each point, of the daily $\overline{u}$ values for each month. In November the variance in the USMM is rather similar to that in the UKMO, with the springtime descent of the southern jet as one maximum and the variance on the axis of the northern jet as the other. Variance in the Northern Hemisphere increases in subsequent months; the largest variance in wind occurs near 1 hPa in months with a sudden

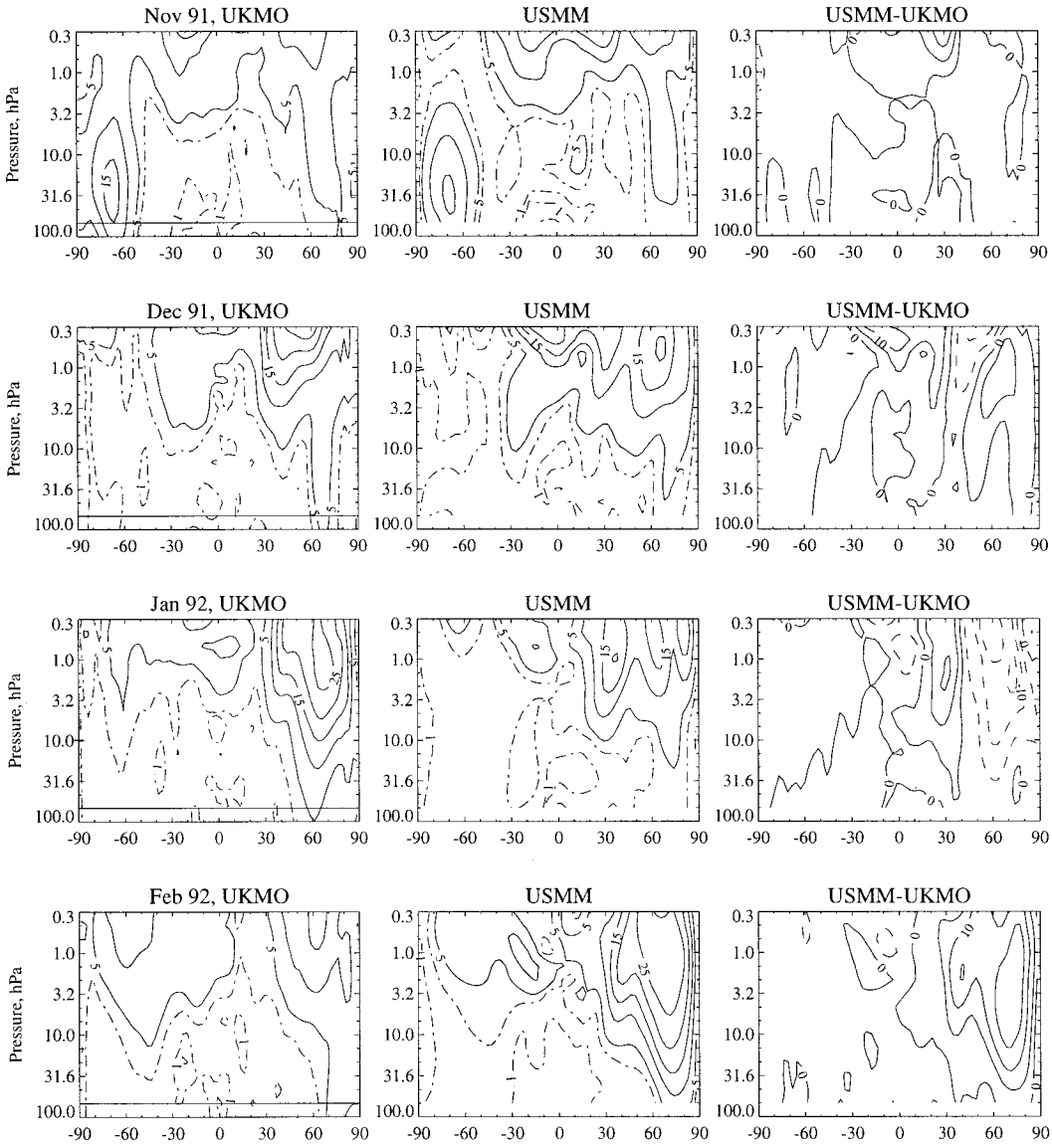

FIG. 2. Standard deviation of daily zonal mean $\overline{u}$ about the monthly mean $\overline{u}$ for November 1991 through February 1992 for UKMO (first column), USMM (second column), and the difference (third column). Contour interval 5 m s^{-1}; broken curves in the first two columns show 1 and 3 m s^{-1} contours.

warming, namely January 1992 in the observations and February in the USMM. For these months the difference between the USMM and UKMO is large at high latitudes. The largest variance in $\overline{T}$ occurs a bit lower than the largest variance in $\overline{u}$, near 6 hPa.

Noting that the largest variance is usually in the Northern Hemisphere, we turn our attention to the Northern Hemisphere and the time-dependent behavior of $\overline{u}$ in the middle stratosphere, at 10 hPa (Fig. 3). O'Neill et al. (1994) and Rosier et al. (1994) noted that the main features of stratospheric flow during the winter 1991–92 were a stable and vertically aligned vortex in early winter and a minor warming in mid-January, during which the vortex developed a tilt. Figure 3a resembles Fig. 2 of O'Neill et al. (1994) for the same winter. For the first several weeks of the simulation, the overall behavior in the model is similar to observations (differences generally less than 10 m s^{-1}) north of 40°N, with a gradual increase in maximum wind speed and a sharpening of the wind gradient equatorward of the jet. Temperature differences at this time (not shown) are very small, usually less than 4 K.

After the observed minor warming, which occurs about 12 January, zonal winds remain weak until summer easterlies appear (in mid-March, not shown). But in the USMM, the vortex remains much too strong for most of the period from mid-January to the end of the run on 29 February. (We have also run the USMM at

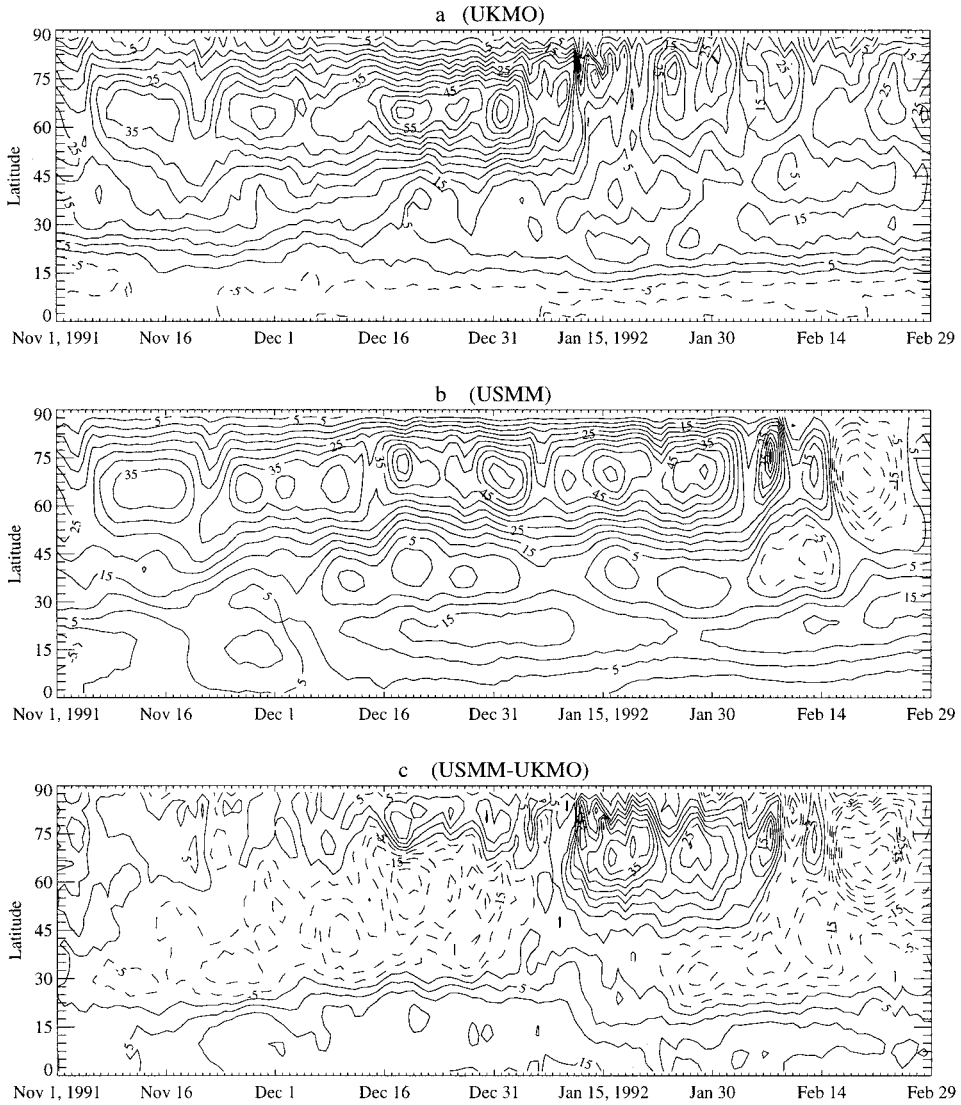

FIG. 3. Zonal mean zonal wind at 10 hPa for (a) UKMO analyses, (b) the USMM, and (c) the difference (b) minus (a). UKMO output has been interpolated to the USMM horizontal grid for plotting.

lower resolution from early November until the end of April, and most of the features before the end of February were similar to those described above. This run successfully reproduced many features of the final warming in March, including the timing and equatorward spread of easterlies.) In mid-February, however, the USMM produces a major warming that extends into the lower stratosphere and has no counterpart in the observations. The temperature rises by 44 K in 3 days and $\overline{u}$ reverses. In section 7 we will examine the observed January warming and the model's February warming.

For a closer look at events in high latitudes, we show height–time plots of (area-weighted) mean temperature north of 60°N (Fig. 4). At the beginning of the run the USMM temperatures above 1 hPa rise rapidly even as the UKMO temperatures fall, leading to large differences; after the assimilation was restarted for 7 December, the UKMO temperatures more closely resemble the USMM. In mid-December, observed temperatures briefly increase over the depth of the polar stratosphere, and the USMM does well at simulating this event. But beginning in the final days of December, UKMO temperatures gradually increase, then diminish slightly before the sudden warming. The USMM produces nothing to match these changes, and differences between the two exceed 40 K. In February, though, the USMM follows suit with a warming of its own, which first erases and then reverses the temperature differences between the USMM and the UKMO. At the end of the run, differences are very close to zero.

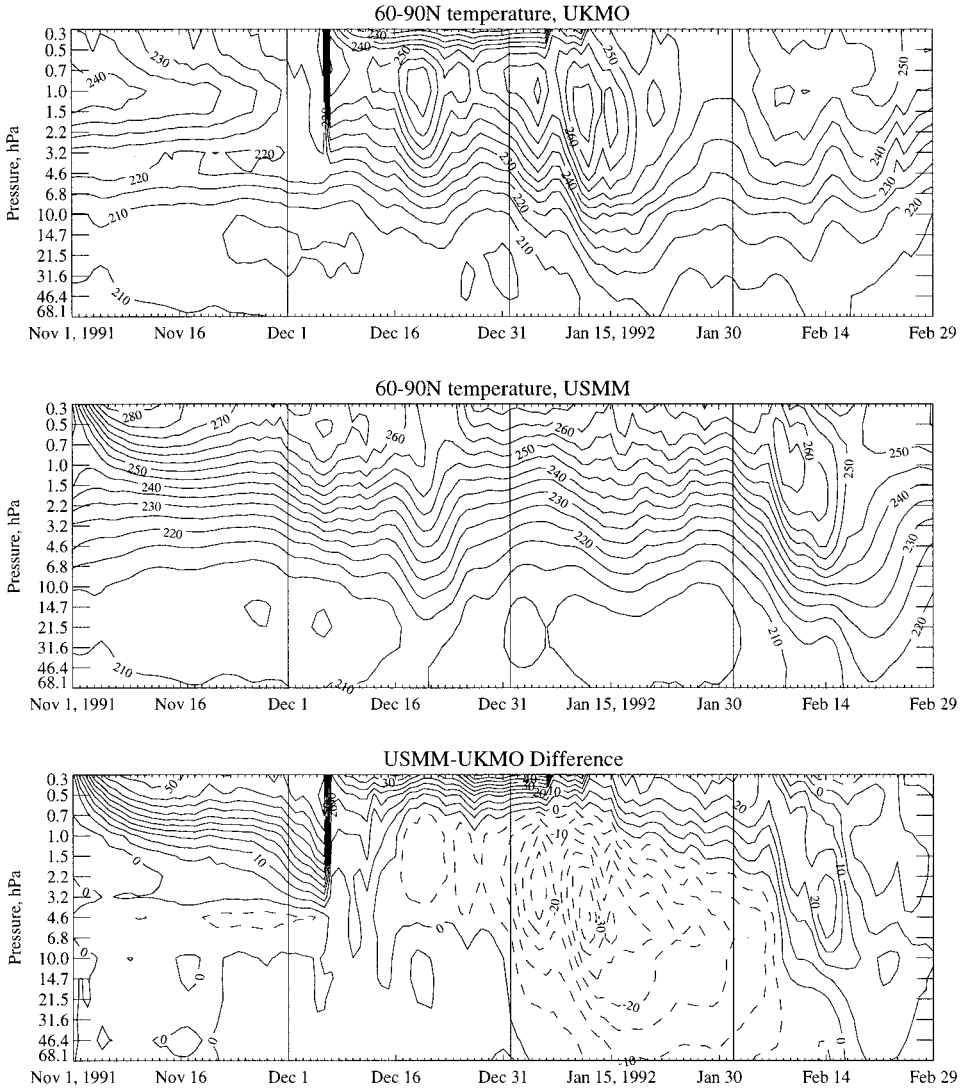

FIG. 4. Average polar temperature (60°–90°N, area weighted) for (a) UKMO, (b) USMM, and (c) the difference. The discontinuity in December was caused by numerical problems in the UKMO assimilation; see section 3 for details.

b. Wave diagnostics

The lower boundary (geopotential height) forcing for the three largest zonal waves during the 1991–92 winter is shown in Fig. 5. Wavenumber 1 amplitudes are usually larger than wavenumber 2 and 3 amplitudes, and the latitude of the maximum decreases slightly with wavenumber from about 65° for wavenumber 1 to about 60° for wavenumber 3. Amplitudes are highly variable in time, but amplitudes of different wavenumbers tend to be negatively correlated; note, for example, the peaks during January of wavenumber 1 on the 9th, wavenumber 3 on the 20th and wavenumber 2 on the 24th. By contrast, Manney et al. (1991) found that wave 1 and 2 amplitudes in the Southern Hemisphere were sometimes positively correlated and sometimes negatively correlated. In Fig. 5d the vertical component of the EP flux, F_z [see (2)], is shown. The maximum generally occurs somewhat equatorward of the largest wave amplitude. The largest peak in F_z occurs on 12 January, just after the peak in wave 1 amplitude. The peak in early December coincides with a lull in wave 1 amplitude and a peak in wave 2 amplitude. At times F_z is negative, mostly at high latitudes.

Figure 6 shows the amplitude of zonal wavenumber 1 for the USMM run and the UKMO data, at the latitudes closest to 65°N, where peak amplitudes generally occur (see, for example, Randel, 1992). There are at least five periods when wave 1 amplitude is elevated, each more coherent in the USMM simulation than in the UKMO data: around 5 November, 22 November, 15 December, 10 January (associated with the minor warming), and 9 February. The first three of these are reasonably well

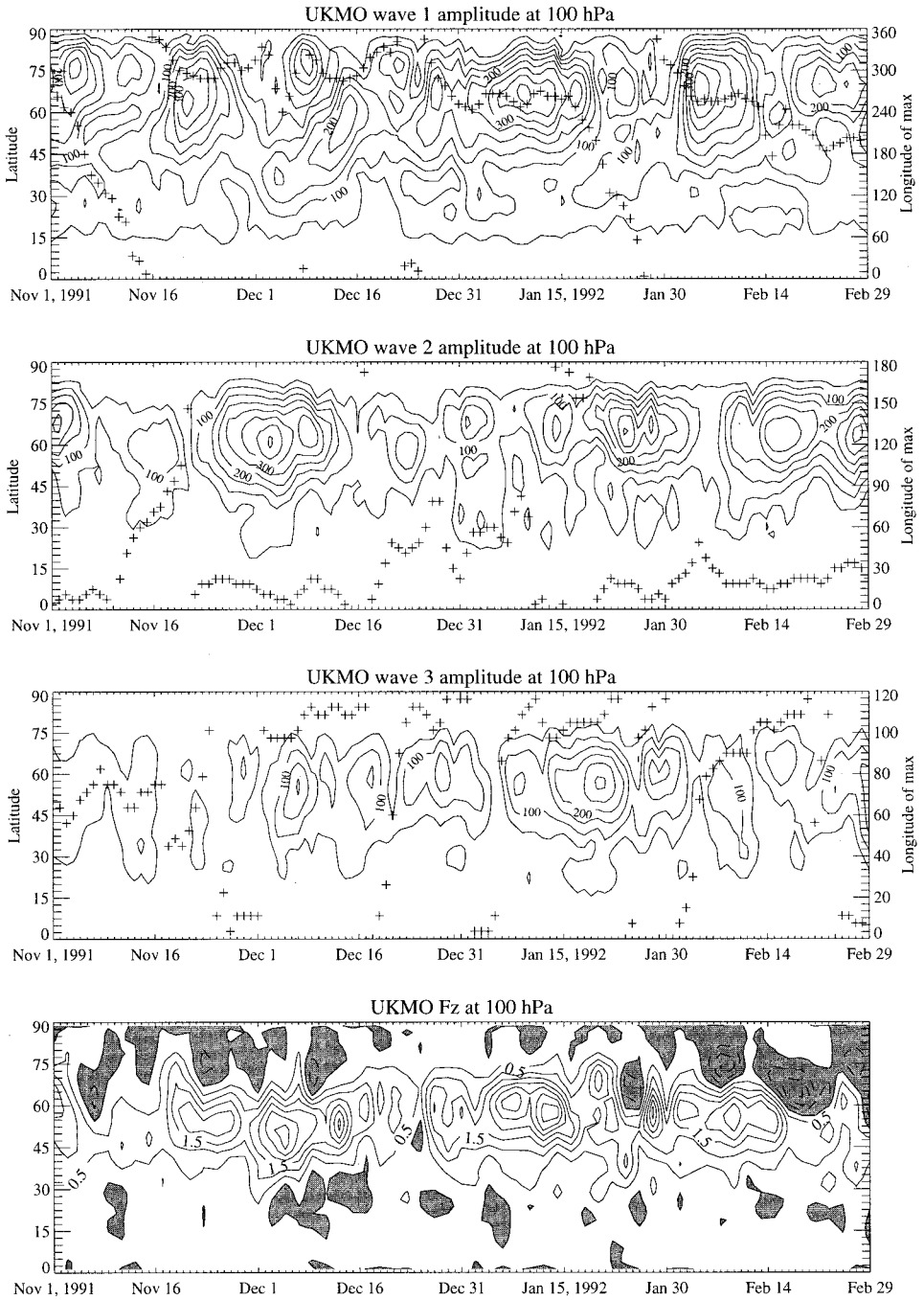

FIG. 5. Amplitude of geopotential height at 100 hPa from UKMO data for zonal wavenumber (a) 1; (b) 2; (c) 3. The "+" symbol indicates the longitude of the peak amplitude in each wavenumber (see right-hand axis). (d) The vertical component of EP flux scaled to the nearest factor of 10.

simulated by the USMM in the upper stratosphere, but the one in December persists too long in the lower stratosphere. The one in January is also reasonably well simulated, though it is larger than observed, occurs a few days late, and fails to result in a wind reversal in the middle stratosphere. The third period is of much greater amplitude in the USMM than observed, and as noted, is related to a major warming in the USMM that had no counterpart in the UKMO data, though in much of February the observed vortex was also distorted (see section 5c). After that, the amplitude of wave 1 in the USMM drops abruptly.

The amplitude of wavenumber 2 (not shown) is considerably smaller than that of wavenumber 1, with more

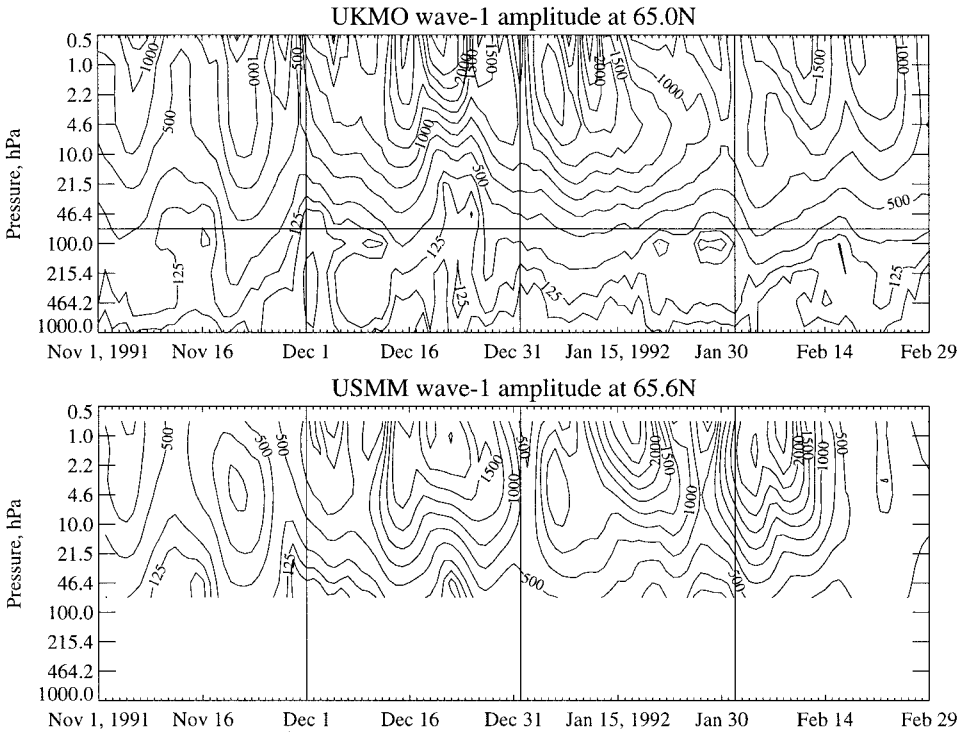

FIG. 6. Amplitude of geopotential height, zonal wavenumber 1, at 65°N for (a) UKMO and (b) USMM. Contour interval is 250 m, and the 125-m and 62.5-m contours are also shown. Vertical bars divide the months and the horizontal bar in (a) denotes the lowest level of USMM data plotted in (b).

frequent peaks. After the first month, when the USMM matches the UKMO fairly well, the USMM's performance at simulating wavenumber 2 seems to be much worse than for wavenumber 1; peaks in wavenumber 2 in the USMM in early December and mid-February do not correspond with peaks in the UKMO.

Another way of viewing wave activity is with the EP flux. Typically EP flux vectors turn equatorward with height in the middle stratosphere, but on some occasions they point upward and poleward (e.g., Dunkerton et al. 1981) in what McIntyre (1982) terms ''focusing'' of the waves. Under these conditions, upward wave propagation can lead to a warming. In Fig. 7 we show the equatorward component of the EP flux ($-F_\phi$) which indicates not just the magnitude of wave activity but (to the extent that WKB theory holds) also the direction in which the waves travel. Most of the time, peaks in F_ϕ occur at about the same time and with similar magnitude in the USMM as in the UKMO. South of 60°N, waves almost always propagate equatorward, with occasional very weak poleward components north of 60°N; but before and during the minor warming in mid-January, the magnitude of F_ϕ (and that of F_z as well) increases dramatically in the UKMO and indicates greater poleward propagation north of about 60°N. During this time F_ϕ for the USMM also indicates poleward propagation, though somewhat weaker; the main difference lies at lower latitudes, where F_ϕ is small in the USMM. In February, the USMM and UKMO both show strong poleward propagation at the time when the USMM produced a major warming. At 10 hPa and above (not shown), neither the UKMO nor the USMM exhibits poleward or downward propagation, but they no longer disagree on the magnitude of F_ϕ at midlatitudes in January.

c. The polar vortex

At 1 hPa, the observed vortex is fairly broad and quiescent until mid-December, when the first of four traveling anticyclones appears. These anticyclones have an average life cycle of about 10 days and tend to form around 90°E, intensifying as they travel eastward, and decay between 180° and 135°W. After each one, the vortex is slightly smaller and its edge sharper. At 10 hPa, the Aleutian high appears at the end of November and remains in place throughout the period studied here, apart from two brief episodes when it weakens and moves 45° longitude away from its usual position. Each time an anticyclone passes over the Aleutian high, the high strengthens and displaces the vortex somewhat (Fig. 8, third row, first three columns), warming high latitudes; these events can also be seen in Fig. 4 (mid-December, two in early January including the minor warming, and one in early February).

The behavior of the vortex and anticyclones in the

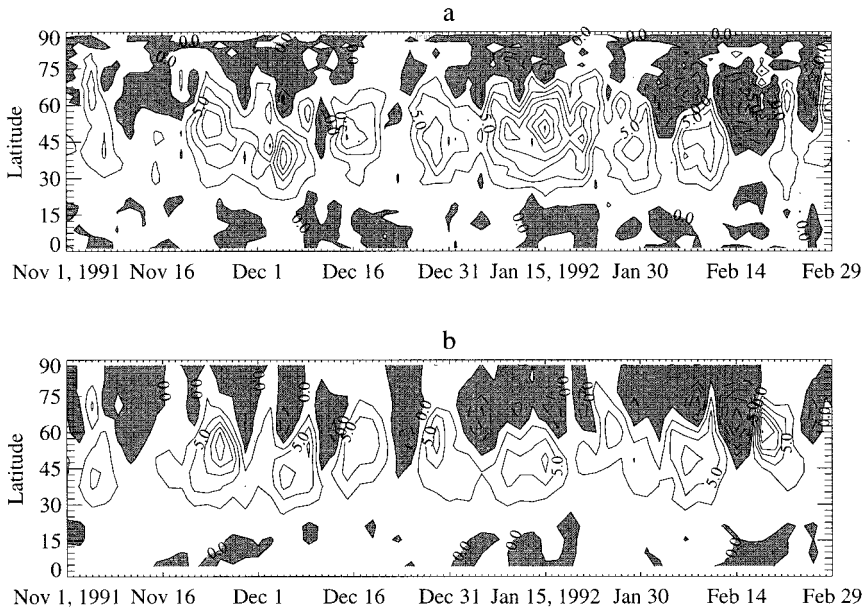

FIG. 7. Equatorward component of EP flux vectors $-F_\phi$ near 30 hPa, scaled to the nearest factor of 10, for (a) UKMO and (b) USMM. Shading indicates positive (poleward) values of F_ϕ.

USMM is rather different. At 1 hPa, three traveling anticyclones appear before the end of December, with a life cycle somewhat shorter and shifted east about 45° from the observed. The third of these (Fig. 8, first column) coincides with the mid-December warming (Fig. 4) that was also observed. But subsequent anticyclones in January (Fig. 8, third column) are stationary, and at 10 hPa the Aleutian high is much weaker than observed and is shifted to the east (second column). For the second half of January and all of February, the observed vortex remains fairly weak and distorted at both levels. But in the USMM, the vortex at 1 hPa strengthens and moves back to the pole during the second half of January. During the first half of February the vortex in the USMM becomes distorted at both levels as anticyclones grow, culminating in the dramatic rise in temperature of 8–11 February (Fig. 4) and in the appearance of easterlies on 15–19 February (Fig. 3). At this time (Fig. 8, fourth column) the vortex at 1 hPa is more distorted than the observed vortex, and even splits.

In order to emphasize the vertical and temporal variations of the vortex, we turn to the vortex-displacement diagnostic (Fig. 9). It can be interpreted by imagining a polar stereographic plot with the Greenwich meridian at the bottom; the tail of the vector is at the North Pole and the head points to the vortex center. The vortex (observed and modeled) during the 1991–92 winter is virtually always displaced toward the longitude sector within 90° of the Greenwich meridian, so that the vortex-displacement vectors point down. In the UKMO data, there are frequently large vertical differences in the position and displacement of the vortex center. Note, for example, the 180° phase shift on 1 December between the 14.7- and 21.5-hPa levels. In the USMM, by contrast, vertical variations on a single day are much smaller and smoother except at the height of the warming on 17 February. The jumps in the UKMO (and the one in the USMM on 20 February) are sometimes due to the presence of two or more minima (see Fig. 8) whose relative depth may change slightly with time or height. But the vortex displacement vectors may indicate a fundamentally weaker connection between vertical levels in the UKMO data than in the USMM. Both the vortex and anticyclones (see Fig. 8) tend to be barotropic in the USMM but more baroclinic in the UKMO data; the dynamical significance of this is that waves that tilt westward with height are more efficient at transporting heat poleward.

In the UKMO data, large vortex displacements (toward the Greenwich meridian) develop in the upper stratosphere at the end of December, initially in connection with one of the traveling anticyclones. At lower levels there are at that time modest displacements toward 90°E, and there is an abrupt transition between the upper and lower regimes. Large displacements descend with time from 2.2 hPa on 28 December to 22 hPa on 15 January, and on 18 January, large displacements are the rule at all levels. As noted in the previous paragraph, such abrupt transitions are sometimes due to the presence of two or more minima, but here the vortex structure really is different above and below the transition level. The transition level seems to delimit the influence of the growing Aleutian high, whose influence spreads downward until the vortex is displaced well off the pole (about 24°) over the entire depth of the stratosphere, with a marked westward tilt (with height) of nearly 90°;

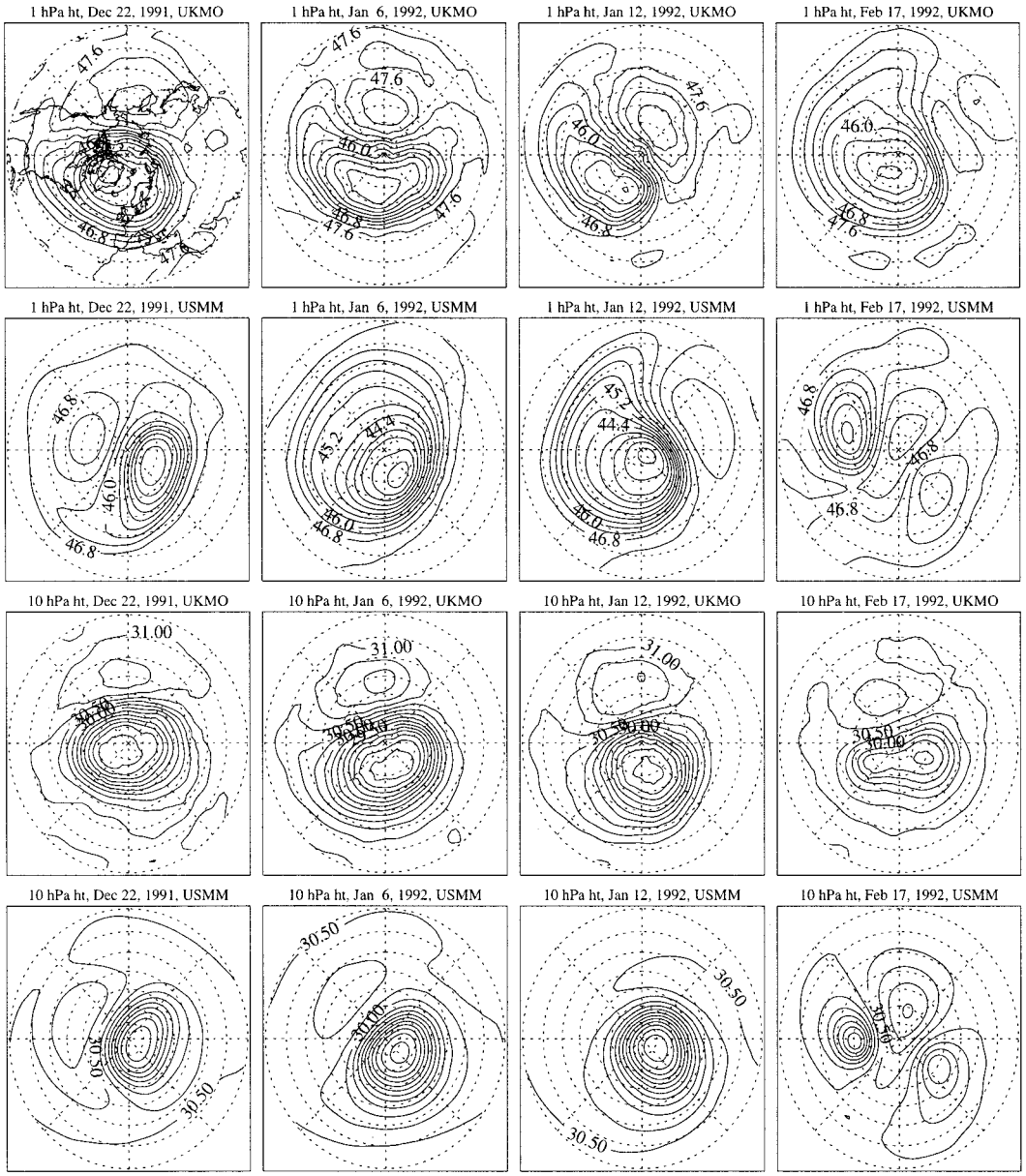

FIG. 8. Geopotential height on 22 December 1991 (first column); 6 January 1992 (second column); 12 January 1992 (third column); and 17 February 1992 (fourth column). Top eight plots, 1 hPa; bottom eight plots, 10 hPa. First and third rows, UKMO data; second and fourth rows, USMM. Lowest latitude shown is 20°, and circles are at 10° intervals. Continental outlines are shown in the top left plot for reference.

this tilt was noted by O'Neill et al. (1994). In February, large displacements are seen again, but the vortex is so weak especially at lower levels that these displacements are not as meaningful.

The failure of the USMM to represent the January warming is evident. The vortex is seldom displaced by more than 12°, though in mid-January the longitude of the vortex center at upper and lower levels is approximately correct at 0° and 90°. The development of the February minor warming in the USMM shares some characteristics with the observed January minor warming: upper levels appear to be disturbed first and there is a roughly 90° tilt.

Another useful shorthand way to display vortex behavior is the PV area diagnostic (Fig. 10; see section 3c for details). In early winter the meridional gradient of PV is nearly uniform, but in December the highest PV value increases and the gradient steepens as PV contours bunch up at around 60°. In the UKMO warming in mid-January, the highest values drop sharply and PV isopleths north of about 50° shift poleward; there is subsequently little change in the meridional gradient of

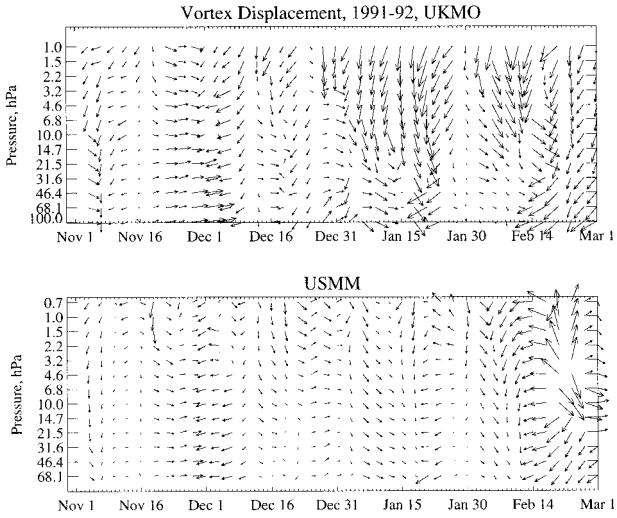

FIG. 9. Time series of vectors whose length and direction indicate the colatitude and longitude of the vortex center, as defined by a hemispheric minimum in geopotential, for the 1991–92 winter. Top panel, UKMO analyses; bottom panel, USMM simulation. Longest vector is about 40°.

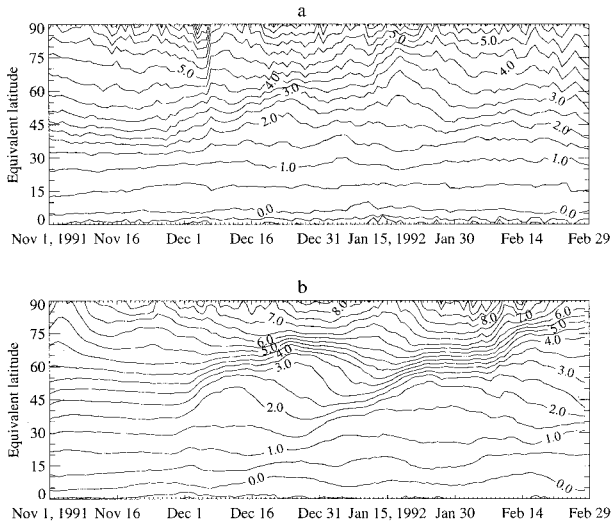

FIG. 10. Area, expressed as equivalent latitude, enclosed by the indicated PV contours on the 1400-K surface, for (a) UKMO and (b) USMM.

PV. In the USMM, however, the meridional gradient of PV becomes much stronger in late December and remains so until the warming in February, when the gradient becomes very weak and the high PV values disappear. For a time in early January, the vortex weakens and grows a bit. By the end of the run the PV field has a very weak gradient and the vortex has all but disappeared, much as in the UKMO data.

6. Description of observed and modeled 1994–95 winter

a. Comparison of zonal mean winds and temperatures

For the 1994–95 winter (Fig. 11), the USMM does a somewhat better job at simulating the mean structure of the jet than it did in 1991–92, but it still produces a sloping easterly jet in the summer subtropical upper stratosphere. In the Tropics, the distribution of $\overline{u}$ in the USMM is similar to $\overline{u}$ for 1991–92, with a lobe of westerlies in the lower stratosphere, but now $\overline{u}$ in the UKMO also has a lobe of westerlies. Apparently the USMM has a persistent westerly bias there, which coincided better with the phase of the QBO in 1994–95, leading to smaller differences in $\overline{u}$. The warm bias at the stratopause now extends to the South Pole, and is statistically significant in the Tropics. Temperature differences in the lower stratosphere are somewhat smaller than in 1991–92 but the differences are statistically significant over a greater range of points. For 1994–95, approximately 70% of points in the latitude–height plane have temperatures within 5 K, compared to 50% for 1991–92. The same percentages apply to wind differences less than 5 m s^{-1}. In the polar lower stratosphere, the winter of 1994–95 was one of the coldest on record, especially in December and March (Zurek et al., 1996),[2] though in the seasonal mean (Fig. 11) it does not appear much colder than 1991–92 (Fig. 1).

The distribution of standard deviation of $\overline{u}$ in November (not shown) is quite similar in the UKMO and USMM, with somewhat larger values at northern high latitudes. In December the USMM has too little variance in the midlatitude upper stratosphere, largely due to events at the end of the month that will be discussed shortly. In January (Fig. 12), variance is large in both the UKMO and the USMM because of the sudden warming, and in contrast to January 1992 (Fig. 2), differences are rather small.

Turning now to the zonal mean flow in the middle stratosphere (Fig. 13), if the winter of 1991–92 was characterized (at least in the UKMO data) by a single event that divided two different regimes, the winter of 1994–95 could be characterized as a single regime, namely a well-established vortex, interrupted by a complex minor warming beginning in January. In late December the observed and modeled winds weaken slightly, then intensify as the meridional gradient on the equatorward edge of the vortex sharpens. In the UKMO data, but not the USMM simulation, the temperature at high latitudes (Fig. 14) rises about 15 K at that time in most of the stratosphere, then diminishes again.

In mid-January the minor warming begins. The appearance of easterlies on 20 January follows a decline that begins on 17 January. (As explained in section 7, this event narrowly fails to qualify as a major warming.)

[2] The winter of 1995–96 was even colder overall (Manney et al. 1996a; Naujokat and Pawson 1996).

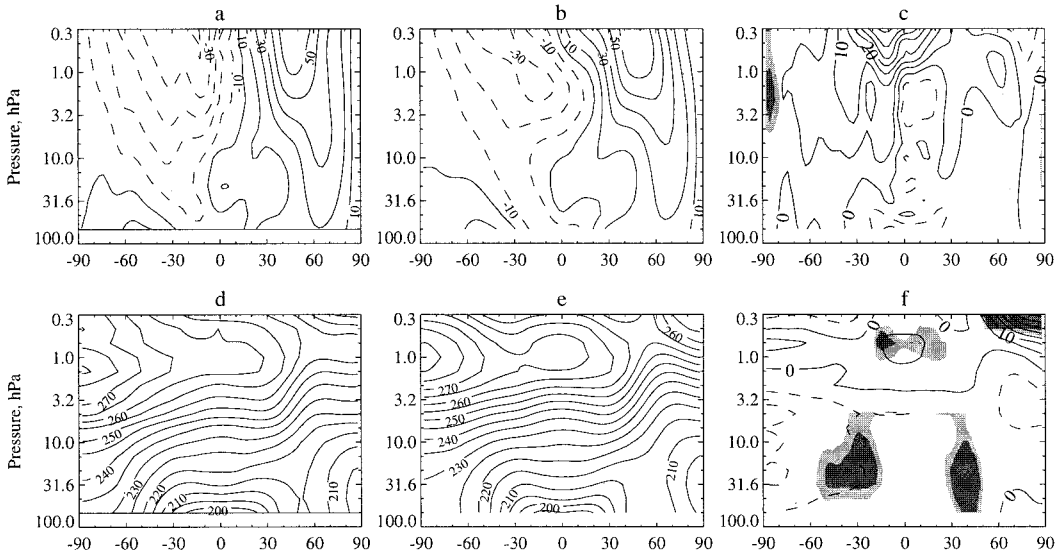

FIG. 11. Zonal mean zonal wind $\overline{u}$ and temperature $\overline{T}$ for November 1994–February 1995. (a) Observed (UKMO) and (b) modeled (USMM) $\overline{u}$; (c) difference in $\overline{u}$, USMM − UKMO. (d) Observed and (e) modeled $\overline{T}$; (f) difference in $\overline{T}$, USMM − UKMO. Statistically significant differences are shaded as in Fig. 1.

Westerlies return for several days in late January, but by 31 January the zonal mean wind is again easterly. This warming was unusual in two respects: 1) the wind reversal occurred in two stages, with westerlies returning for a few days; and 2) the depth of the warming, with easterlies and warming extending into the troposphere. All of the features in both winds and temperature are well simulated by the USMM, except during the period 25–30 January, when polar temperatures drop and the westerlies are too strong. At the end of the simulation, differences are again small.

To evaluate the model's overall performance, we compare the global mean temperature (between 68 and 0.68 hPa) in the model and the UKMO data for both winters (Fig. 15). The global mean temperature is almost always lower in the USMM, a bias that is worst during the missed warming of January 1992. During both winters, there is an initial adjustment of the temperature field; the rms temperature difference rises sharply, then levels off to a fairly steady value. This steady value is about 6 K for 1994–95 and about 8 K for 1991–92 (apart from the aberration caused by the problem with UKMO data before 7 December 1991), even during the January 1992 warming that the model missed. Both the global mean temperature difference and the rms temperature difference are almost always smaller in 1994–95.

b. Wave diagnostics

Compared to 1991–92, the wave amplitudes of 100-hPa geopotential height (Fig. 16) are generally much greater in 1994–95. (In fact, the peak amplitude of wavenumber 2 on 20 January 1995, exceeds the peak amplitude of wavenumber 1 in 1991–92.) In 1994–95, wave 1 amplitude is largest in late December (with a peak on the 24th), late January (also with a peak on the 24th), and mid-February (with a peak on the 10th). Wave 2 amplitude is largest in early and mid-January, with a peak on the 20th. Wave 3 peaks are small (mostly 200 m or less) and occur very close to peaks of wave 2 (in early and mid-January) and wave 1 (in early February). By contrast, recall that in 1991–92 the peaks of one

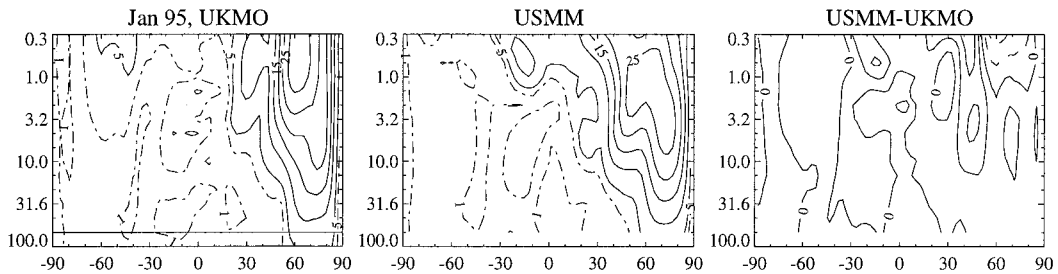

FIG. 12. Standard deviation of daily $\overline{u}$ about the monthly mean $\overline{u}$ for January 1995, and the difference between USMM and UKMO standard deviations. Contours as in Fig. 2.

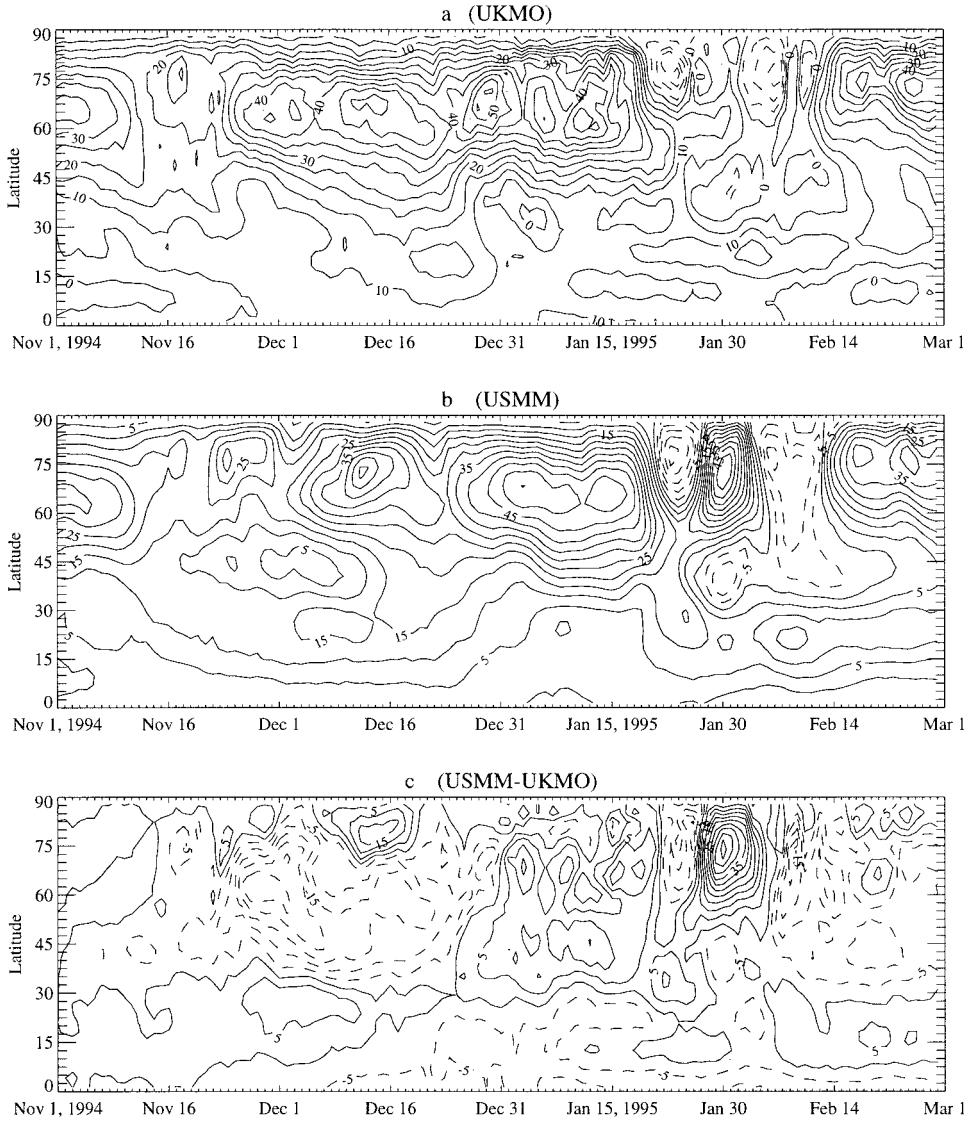

FIG. 13. Zonal mean zonal $\overline{u}$ at 10 hPa for (a) UKMO, (b) USMM, and (c) the difference (cf. Fig. 3 for 1991–92).

wavenumber occurred when the amplitudes of other wavenumbers were small. The vertical component of EP flux (Fig. 16d) reaches slightly higher positive values and much lower negative values than in 1991–92. As before, the peaks are sometimes roughly coincident with peaks in wave 1 (the December peak) and sometimes with wave 2 (the January peak), but the peak during the first two days of February occurs when waves 1 and 3 are small but growing and wave 2 is declining.

Cross sections of wave amplitude at 65°N (Fig. 17) show considerable differences between the UKMO and the USMM. In the UKMO analyses, significant peaks in wave 1 amplitude in the stratosphere occur in mid-November, late December, and late January, with large amplitudes maintained from mid-December to mid-February. Wave 1 amplitudes reach a peak of 3069 m at 1 hPa on 31 December 1994, considerably greater than at any time in 1991–92. In the USMM simulation, some peaks occurred at about the same time (Fig. 17b), but the large peak in late December at 1 hPa is missing (consistent with the lack of warming then—see Fig. 14), and is followed by a period of weak wave 1 amplitude (though stronger wave 2 amplitude) for about the first two weeks of January.

Harwood (1975), Leovy and Webster (1976), Manney et al. (1991), and Farrara et al. (1992) showed that in the Southern Hemisphere, eastward phase propagation of wavenumbers 1 and 2 is a common occurrence in the middle stratosphere, especially when wave amplitudes were large or growing; in some instances the phase progressed through 360° longitude in about 20 days. In Figs. 5 and 16, the longitude of each wave's maximum

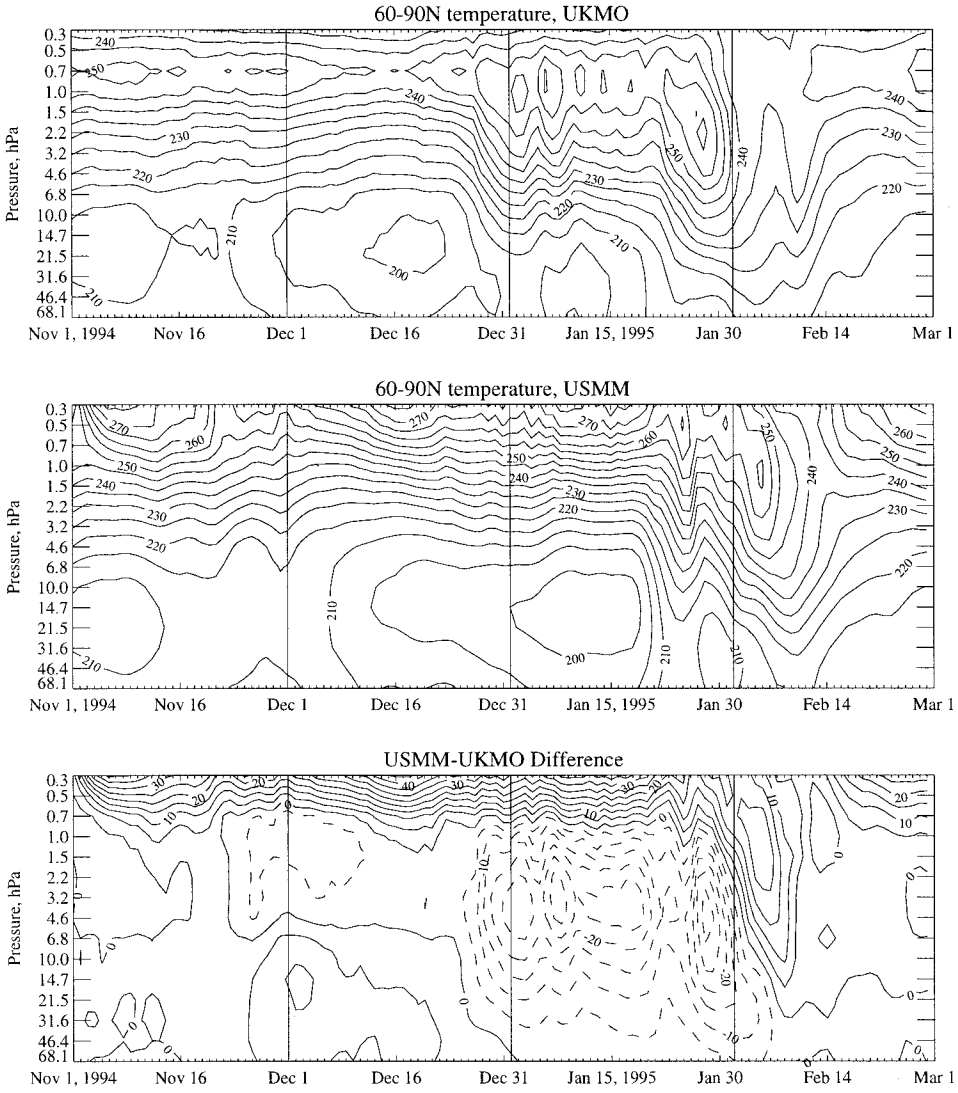

FIG. 14. Average polar temperature (cf. Fig. 4 for 1991–92).

at 60°N is indicated by a "+" symbol; eastward progression for more than a few days is very unusual. There are, however, a number of instances of westward progression (1–20 November 1991, 16 January–3 February 1992, and most of February 1995) of wave 1, and a few instances of prolonged eastward progression of wave 2 (10–23 November 1992) and wave 3 (9–31 January 1995). Manney et al. (1991) noted that in the Southern Hemisphere, regular eastward progression was much less common and much shorter lived below 100 hPa than above 100 hPa, in agreement with our finding for these northern winters.

But what happens at higher levels? Figure 18 shows plots of wave amplitude and phase for waves 1–3 for UKMO data at 10 hPa. For both waves 2 and 3, eastward progression is more common than at 100 hPa. In the USMM (Fig. 19), however, eastward phase progression of waves 2 and 3 is not as common as in the UKMO. For wave 1, phase progression in both directions is more common in the USMM than the UKMO; for example, note the eastward progression of 1–24 December and the westward progression of 25 December–25 January. In 1991–92 (not shown), eastward phase progression in the stratosphere is less common than in 1994–95.

To judge the performance of the USMM at simulating the phase of waves, we show in Fig. 20 a quantity defined as

$$\overline{\cos m[\lambda_m^{\mathrm{USMM}}(t) - \lambda_m^{\mathrm{UKMO}}(t)]},$$

where m is the zonal wavenumber (included because the maximum phase difference drops as $1/m$), $\lambda_m(t)$ is the phase of wavenumber m in radians at a given latitude (60°), and the overbar indicates a time average. This quantity, like a correlation, can range from -1 to 1. From the figure it is apparent that the accuracy of phases simulated by the USMM drops with height and that

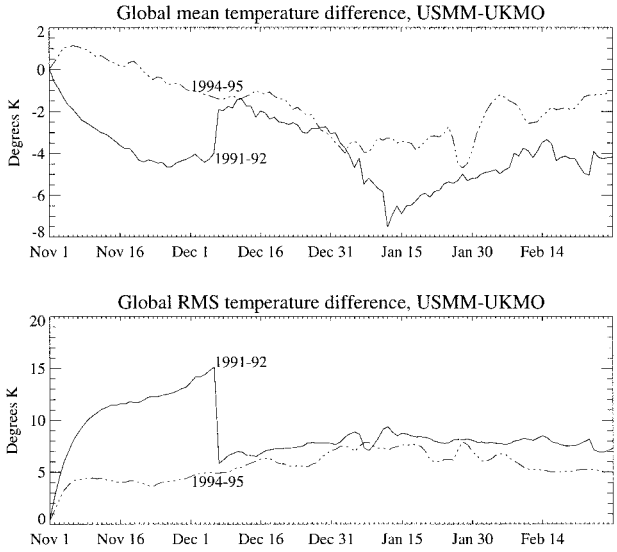

FIG. 15. Global (a) mean and (b) rms stratospheric temperature difference between USMM and UKMO. Area weighting, but not density weighting, has been applied.

phase errors of $m = 2$ and $m = 3$ are similar, and are significantly worse than phase errors of $m = 1$. There is little difference between the winters in the accuracy of $m = 1$, but the accuracy of $m = 2$ is worse in 1991–92; worse, in fact, than $m = 3$ in much of stratosphere.

Plots of the EP flux component F_ϕ (not shown) for both USMM and UKMO indicate a stronger poleward turning during the January 1995 minor warming than in January or February 1992. The magnitude of F_ϕ in the USMM agrees better with the UKMO than during the January 1992 warming.

c. The polar vortex

Until late December, the vortex in the UKMO data at both levels is distorted only slightly and displaced only slightly from the pole. In the USMM, however, an anticyclone develops in late November–early December (Fig. 21, first column) with an unusual eastward phase tilt of about 120° between 10 and 1 hPa; this anticyclone distorts and displaces the vortex much more than observed. We saw evidence of this disturbance in Figs. 13 and 14; it has no counterpart in the UKMO data. In late December, an anticyclone develops in the UKMO data and the USMM (Fig. 21, second column); at 1 hPa the anticyclone is much weaker and farther south in the USMM simulation (see also Fig. 17). Throughout the month of January, the observed vortex remains distorted at 1 hPa and the Aleutian high remains strong at 10 hPa. The location and strength of both the vortex and the anticyclone are well simulated by the USMM.

As the minor warming develops, the vortex is displaced from the pole and nearly divided by a strengthening Aleutian high (Fig. 21, third column). At upper levels the vortex is distorted, with an arm of vortex air (as is evident in the PV field, not shown) stretching southwestward toward the date line. The USMM matches the shape of the vortex fairly well at both levels. During the period 25–30 January, the unrealistic strengthening of the westerlies in the USMM (Fig. 13) is related to the fact that the vortex in the USMM is stronger and closer to the pole than the vortex in the UKMO data (Fig. 21, fourth column). The vortex remains too strong until it is again displaced from the pole in early February as observed, leading again to easterlies in the zonal mean.

The vortex-displacement diagnostic (Fig. 22) generally confirms that the USMM more faithfully simulated the observed flow during the 1994–95 winter than during the 1991–92 winter (Fig. 9). For most of November, the position of the USMM vortex corresponds well at all levels with the observed vortex. At the end of November, though, as the anticyclone grows in the USMM (Fig. 21, top-left panel), the vortex is displaced into the wrong hemisphere. Small displacements and small differences are the rule throughout December, but at the end of December a robust anticyclone (Fig. 21, second column) in the UKMO data shoves the vortex well off the pole in the upper stratosphere, while a feeble anticyclone in the USMM leaves the vortex relatively undisturbed. In mid-January, at the time of the warming, the simulated vortex behaves very differently from the observed vortex. In this case, though, the vortex-displacement vectors are misleading: inspection of maps of geopotential height shows that the vortex shapes are similar, each with two minima (see Fig. 21, third column), but the minimum at 90°E is deeper in the USMM while the minimum at 10°W is deeper in the UKMO at most levels.[3] In the second half of February the correspondence is again good.

As in 1991–92, in the early stage of the warming the vortex was sheared, displaced toward Europe at upper levels and toward 90°E at lower levels, with a transition that moved downward with time. But this time, the vortex displacement developed simultaneously with the wind reversal; in 1991–92, it occurred almost two weeks earlier.

The PV area diagnostic (Fig. 23) provides another perspective on the seasonal development of the vortex. In the UKMO, the vortex shrinks markedly in early January and again (less dramatically) during the warming in late January. In most of February the vortex is weaker and less well defined than it was in November. Events develop differently in the USMM. During the event near the beginning of December in the USMM, the vortex shrinks and its edge sharpens. Over the next several weeks the vortex grows in strength; it does not

[3] As we have seen, a weakness of the vortex displacement diagnostic is that apparently large differences can result from small differences in the relative height of two distant minima; Waugh's elliptical diagnostics should not suffer from this weakness.

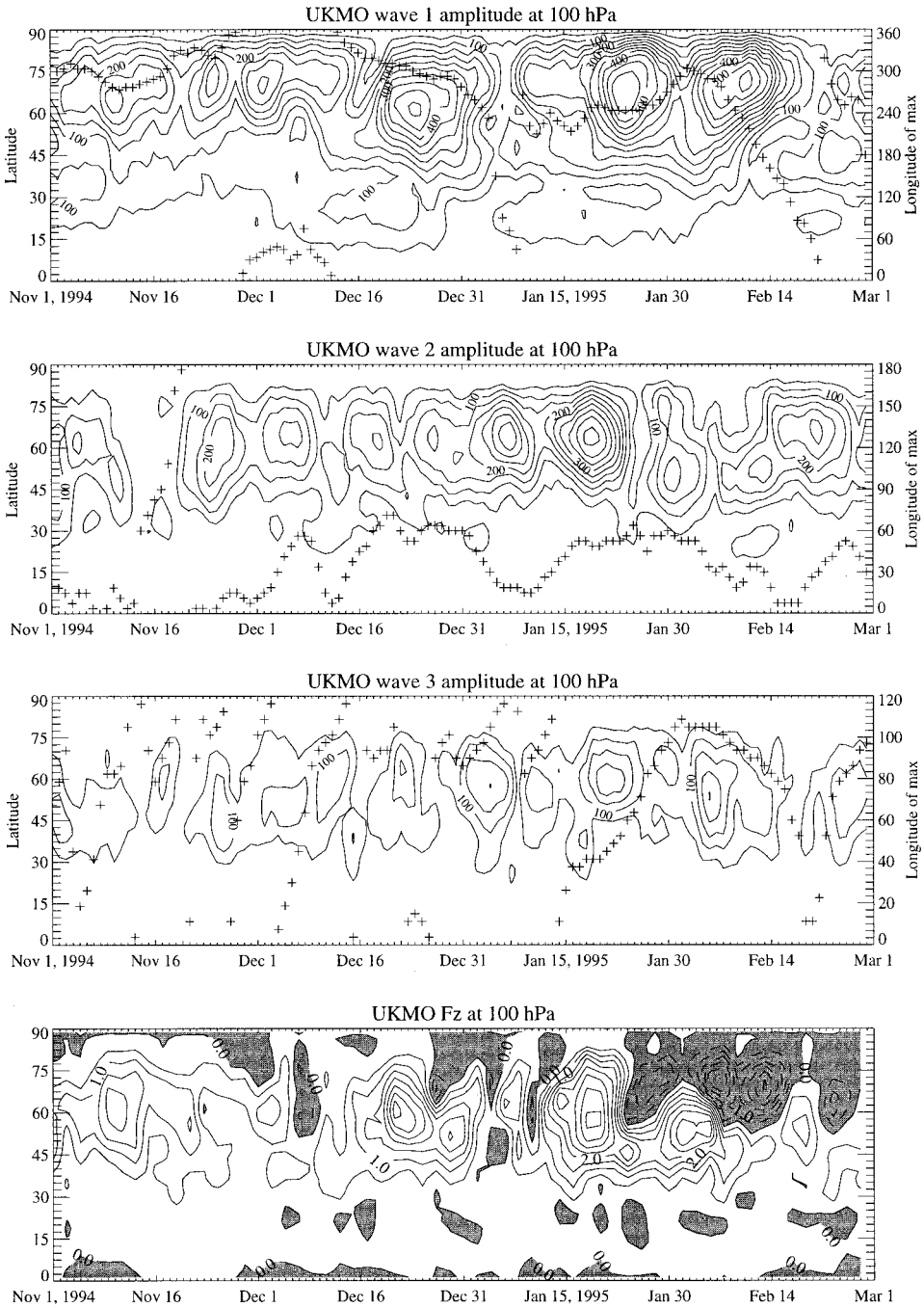

FIG. 16. Amplitude of geopotential height at 100 hPa from UKMO data (cf. Fig. 5 for 1991–92).

shrink as markedly in early January as observed. During the warming, however, the vortex shrinks while retaining its sharp edge (see Fig. 21). By the end of the run, the PV distribution is very similar to that of the UKMO.

7. Sudden warmings

Sudden warmings are perhaps the most dramatic flow event in the stratosphere; in a typical event, temperatures rise by 40 K or more over much of the polar region in just a few days, and the vortex is displaced from the pole and sometimes split apart. Sudden warmings are most frequent and most vigorous in the Northern Hemisphere and, though they do not occur every winter, when they do occur it is generally in January. The World Meteorological Organization (WMO) definition of a ''major warming'' is that at 10 hPa 1) the zonal mean

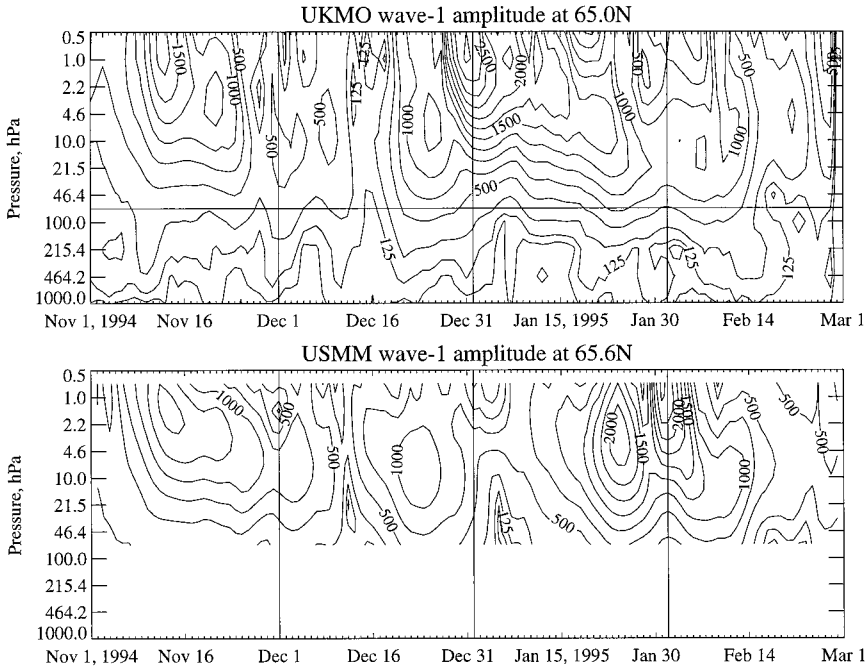

FIG. 17. Amplitude of geopotential height at 65°N; see Fig. 6 for details.

temperature increases from 60°N poleward and 2) the zonal mean wind at 60°N is easterly (e.g., Naujokat and Labitzke 1993). A minor warming fulfills only the first of these requirements. Although the term minor connotes insignificance, minor warmings are often quite significant. Consider the January 1992 event (Fig. 3), from which the vortex never recovered. O'Neill et al. (1994) referred to the January 1992 event as a ''near major'' warming because the wind reversal almost reached 10 hPa at high latitudes. The January 1995 event came even closer to qualifying as a major warming, with a wind reversal coming within 2° of 60°N at 10 hPa; rather than call this event a ''very nearly major'' warming we have called them both minor warmings. The simulated warming in February 1992 qualified as a major warming.

The characteristics of the observed sudden warmings in the two winters were rather different. In 1991–92 the observed warming developed when the third in a series of traveling anticyclones in the upper stratosphere lined up with the persistent Aleutian high in the middle stratosphere. In 1994–95, only one traveling anticyclone appeared in the upper stratosphere and that was a few weeks before the warming. The erosion of the vortex was accomplished largely by the growth of the Aleutian high in the middle stratosphere (Fig. 21), not by the agency of anticyclones in the upper stratosphere. Note that the largest increase in temperature precedes the decrease in wind in 1991–92 (Figs. 3 and 4) but the sequence is reversed in 1994–95 (Figs. 13 and 14).

In many respects, the USMM simulation of the 1994–95 warming was reasonably successful (Figs. 13 and 14), but some notable differences were apparent especially concerning the structure of the vortex. The vortex was observed to split in the upper stratosphere in late January (Fig. 21, fourth column; UKMO data show an anticyclone over the pole[4]), but took a week longer to do so in the USMM (not shown). As is also evident in Fig. 13, the USMM simulated fairly well the two-stage warming with a weakened vortex returning to the pole briefly in late January before being displaced anew in early February by an anticyclone at about 135°W; the location of the anticyclone was well simulated by the USMM, though the vortex itself was somewhat too far west (Fig. 22) and was too strong.

An interesting and unusual feature of this minor warming was the large amplification of wavenumber 3. In the UKMO analyses, it reached a peak of over 600 m at 4.6 hPa on 22 January at about 55°N; the USMM shows similar behavior, with even greater wave amplitudes. During 1991–92, wave 3 amplitudes seldom exceeded 300 m and were considerably smaller than that during the minor warming. This remarkable wave growth did not coincide with the remarkable wave 3 amplitude at 100 hPa (Fig. 16c); the peak at the time of the warming is much smaller than the one on 20

[4] Note the similarity of the observed warming in January 1995 to the USMM warming in February 1992 (Fig. 8).

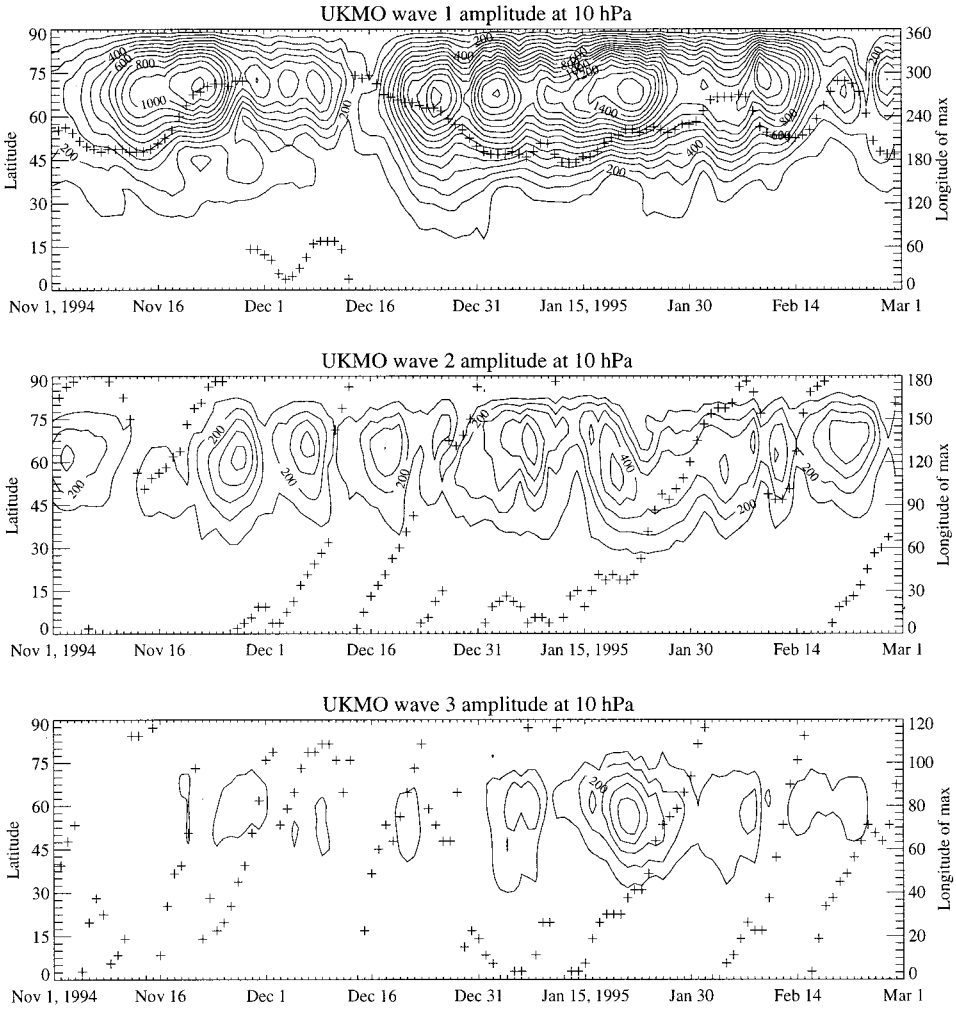

FIG. 18. As in Figs. 16a–c but at 10 hPa.

January 1992 (Fig. 5). We will shortly examine wave growth during the January 1995 warming.

In 1991–92 the model produced no warming in January, when a warming was observed in the real atmosphere, but did produce a warming in February, when no warming was observed; this failure was the greatest puzzle in our simulations. A complete analysis of this failure is beyond the scope of this paper [it could follow Farrara et al. (1992) in constructing simplified initial and lower boundary conditions] but we might speculate that the difference is related to the greater frequency of traveling anticyclones during 1991–92. McIntyre (1982) suggested that a single burst of planetary wave activity is insufficient to cause a warming, but can instead ''precondition'' the stratosphere (shrinking the vortex) so that planetary waves are focused poleward, and the next burst produces a warming. Of the observed and modeled warmings, only the observed January 1995 warming (Fig. 23a) fits this scenario, and only in the upper stratosphere; at lower levels, none of the warming events show evidence of preconditioning. After each traveling anticyclone in December 1991 and January 1992, the observed vortex shrinks a bit, so perhaps the USMM failed to produce the January 1992 warming because its anticyclones were too weak and infrequent to precondition the vortex; Fig. 10 indicates that the vortex was large but weak in early January.

Planetary-scale waves usually propagate upward from the troposphere to the stratosphere (e.g., Fig. 5, or Randel 1987). It would seem reasonable to assume that sudden warmings are a direct response to tropospheric forcing. But there are also instances when wave growth in the stratosphere occurs without any apparent tropospheric forcing (e.g., Manney et al. 1991), and sudden warmings have appeared in models with steady lower boundary forcing, provided the forcing is of sufficient amplitude (e.g., Hsu 1981). Figure 24 shows, for part of the 1994–95 winter, some striking examples of wave growth in the stratosphere that is not related in an obvious way to tropospheric forcing. (Plots of wave am-

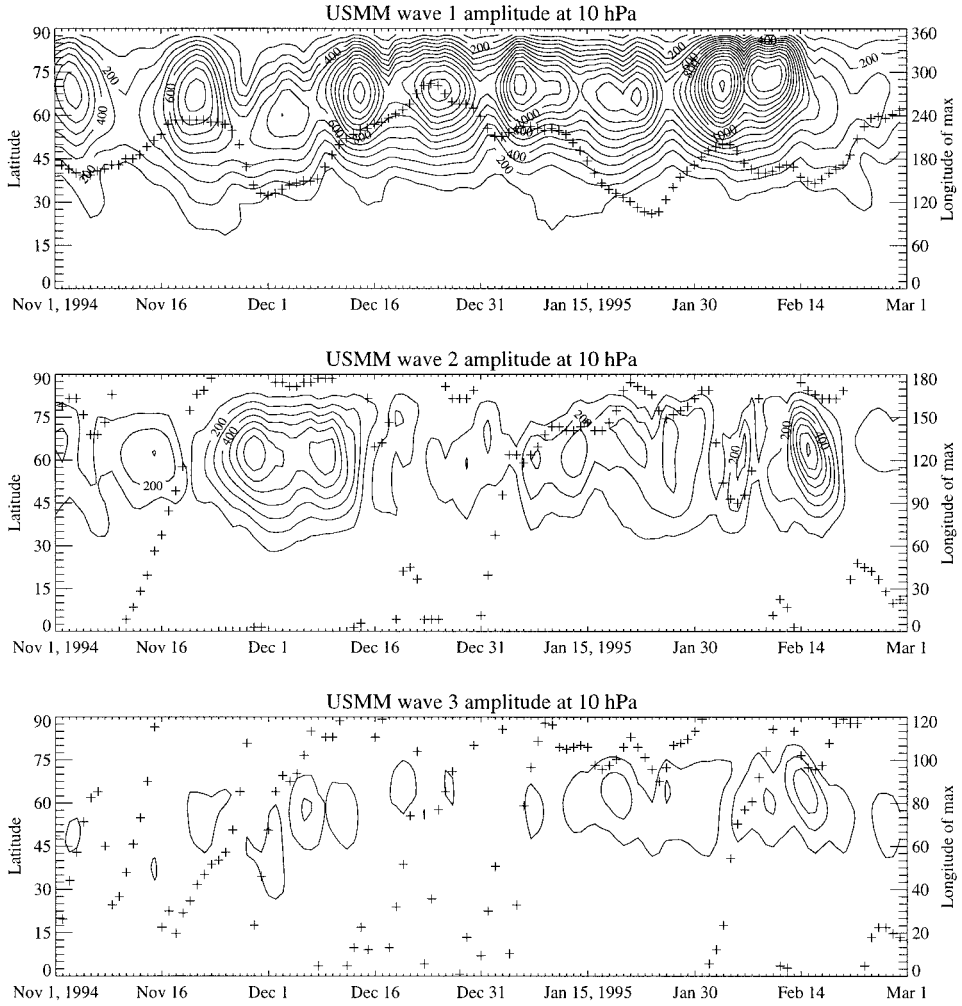

FIG. 19. As in Fig. 18 but for the USMM.

plitude at a certain latitude can leave the reader wondering if wave growth is due to meridional propagation, so we have shown maximum wave amplitude at any latitude for each day.) Bearing in mind McIntyre's (1982) warning that growth of geopotential height waves does not necessarily indicate propagation, we will refer to such situations as ''apparent propagation.'' Focusing first on the UKMO data, we can see a few instances of apparent upward wave propagation: 24–25 December for wave 1, 4–7 and 21–22 January for wave 3. The two wave 2 events appear to develop nearly simultaneously throughout the stratosphere, the second at the time of the minor warming. But on two occasions, 31 December–2 January and 21–24 January, wave 1 growth appears to develop top-down. Note that the wave 1 peak on 24 January (when waves 2 and 3 have small amplitude) corresponds to the advent of downward F_z (Fig. 16), suggesting that the peak at 100 hPa may have been caused by a *downward*-propagating wave that developed in the upper stratosphere or mesosphere.

It is no surprise, then, that the USMM sometimes has great difficulty simulating the observed pattern of wave growth. On some occasions (e.g., 5–6 February for wave 3) waves propagate upward in the USMM but are attenuated in the UKMO data. On other occasions (4–7 January, also wave 3) the reverse is true. And on 24 January, when Figs. 16, 17, and 24 suggest downward propagation of wave 1 in the UKMO data at 100 hPa, the USMM, forced by a wave whose structure is consistent with downward group velocity, can only respond to the wave 1 peak with modest wave growth.

To connect the wave growth considerations to the horizontal, vortex-centered perspective, we construct a scenario that relates the wave 1 forcing of 24 December 1994, with the observed subsequent wave 1 growth. When the upward-propagating wave 1 reaches the upper stratosphere (at around 25 December), it initiates a traveling anticyclone which, upon reaching 180° longitude, becomes phase locked with a weak Aleutian high at lower levels; the intensification of the Aleutian high

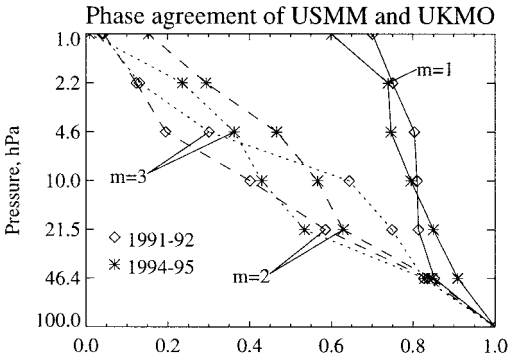

FIG. 20. Phase agreement (see text for definition) between USMM and UKMO wavenumbers 1–3 at 60°N.

develops downward and accounts for the sharp rise in wave 1 around 31 December. In the USMM, however, the large wave 1 amplitudes of 21–26 December are followed by only a small anticyclone at 1 hPa, stationary at about 135°E, and the Aleutian high at 10 hPa never intensifies.

8. Discussion and conclusions

The flow in the stratosphere was significantly different during the two winters described here, although both had a warming in January. In 1991–92, the warming sharply divided two regimes: the vortex was strong before the warming and weak after the warming (Figs. 3 and 8). By contrast, the vortex recovered from the warming rather rapidly in 1995 (Fig. 13). Traveling anticyclones in the upper stratosphere (suggested in the top row of Fig. 8) were common in 1991–92 but not in 1994–95. In both winters, disturbances about two weeks before the warming may have sharpened the vortex edge (Figs. 3, 13, and 23a; less apparent in Fig. 10) and displaced it from the pole (Figs. 9 and 22). The dominant wave during the time of the warming was wave 1 in 1992 (Fig. 5) but wave 2 and wave 3 in 1995 (Fig. 16).

a. Model performance

We have evaluated the USMM's performance at simulating the observed winters in a number of ways, so that we can state its success in quantitative terms. The global rms temperature difference between the USMM and UKMO is about 6–8 K, with the model generally colder than observed (Fig. 15); a notable exception is at upper levels north of 60°N, where the UKMO data are significantly colder (Figs. 1 and 11). Note, however, that a cold bias of several degrees was also found in UKMO data relative to NMC data (Swinbank and O'Neill 1994; Manney et al. 1996b), so the USMM may not be quite as far off the mark as it appears. The USMM does fairly well simulating time-mean winds in the extratropics, but less well in the Tropics. It has a westerly bias—unusual for GCM's and mechanistic models—in the lower stratosphere, and another westerly bias in the lower mesosphere. These biases may have impacts on transient features like sudden warmings at middle and high latitudes, in the same way that the QBO affects the frequency of sudden warmings (e.g., O'Sullivan and Dunkerton 1994). For 1991–92, about 50% of the grid points in the latitude–height plane had a zonal mean temperature $\overline{T}$ within 5 K of the UKMO $\overline{T}$, and about 50% of the grid points had a $\overline{u}$ within 5 m s^{-1} of the UKMO $\overline{u}$. For 1994–95, both percentages were about 70%.

We have also examined the simulation of the three gravest planetary-scale waves. Wave amplitudes in the middle and upper stratosphere are usually similar (see Figs. 18 and 19) but are sometimes markedly different, even when $\overline{u}$ is well simulated (e.g., 1–5 January 1995; see Figs. 17–19 and 24). The phase accuracy degrades sharply with height and wavenumber (Fig. 18–20); wave 2 in 1991–92 was simulated worst. In some cases (e.g., 21–24 January 1995) waves apparently grow internally (Fig. 24) as sometimes occurs in the Southern Hemisphere (Manney et al. 1991); in such situations, the USMM is likely not only to miss the internal wave growth but to respond inappropriately if those waves propagate down to the lower boundary.

In simulating the structure of the vortex, the USMM appears to have difficulty in a few respects. The vortex is frequently too strong (especially when it is very small; see Fig. 8, bottom right), and too barotropic (see Fig. 9). Anticyclones are frequently too weak, too stationary, or have the wrong vertical structure. We have no ready explanation for the excessive strength of the vortex in the USMM, but in USMM simulations at T106 horizontal resolution, the vortex was weaker partly due to faster erosion at the vortex edge and partly due to a wave-breaking event not present at lower resolution (G. Watson 1996, personal communication). On the other hand, in runs of a gridpoint mechanistic model, Beck (1996) found that as resolution increased, the simulated vortex grew stronger. His highest resolution was approximately equivalent to our T42.

The USMM was reasonably successful in capturing the main features of the 1994–95 winter, including the evolution of wave amplitudes and the unusual minor warming of mid-January 1995. This warming was unusual in three respects: 1) the wind reversal occurred in two stages, with westerlies reappearing for a few days (Fig. 13); 2) easterlies and warming extended into the troposphere poleward of about 78° (Fig. 14); and 3) wave 3 apparently played a prominent role (Fig. 24). The USMM reproduced these features well. Its greatest failure during this warming was in restoring the westerlies; as seen from the maps of geopotential height (Fig. 21) and the PV area plot (Fig. 23), this was due to a vortex that was somewhat stronger than observed and that returned more rapidly to a pole-centered position.

Despite the identical formulation of the USMM for

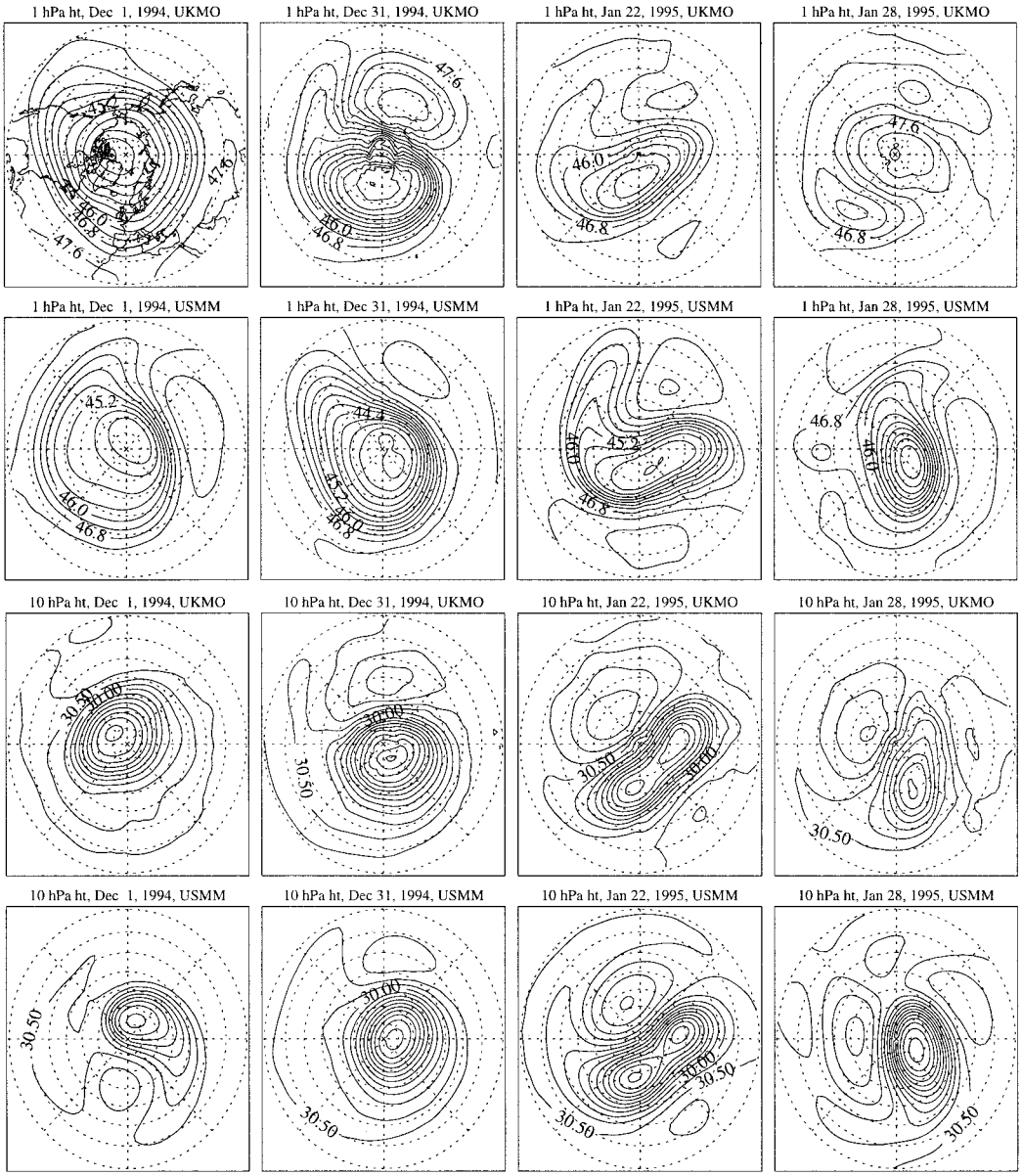

FIG. 21. Geopotential height (as in Fig. 8) for 1 December 1994 (first column), 31 December 1995 (second column), 22 January 1995 (third column), and 28 January 1995 (fourth column).

the two winters, the model performed worse in 1991–92 than in 1994–95. This difference is most apparent in Fig. 3 (cf. Fig. 13), which shows the missed warming of January 1992, and in Fig. 15, in which we see a persistently larger difference from observations in 1991–92 (especially before 7 December 1991, when there were problems with the UKMO data). In the Tropics, the difference in performance stems from the fact that the USMM generally produces weak westerlies in the middle stratosphere, a bias that coincided more closely with the phase of the QBO in 1994–95 than in 1991–92. In high northern latitudes, the model produced a minor warming in January 1995 as observed, but missed a minor warming in January 1992, and produced a major warming in February 1992 when no warming was observed, though planetary-wave forcing was appreciable then (see Fig. 5d).

We offer a few observations in connection with the model's superior performance in 1994–95. First, the character of the forcing at 100 hPa was different; wave amplitudes were much larger in 1994–95 and the peaks occurred closer together in time (see 18–25 January in Fig. 16). The largest wave amplitude for any wave occurred on 25 January 1995, for wave 1, but this was

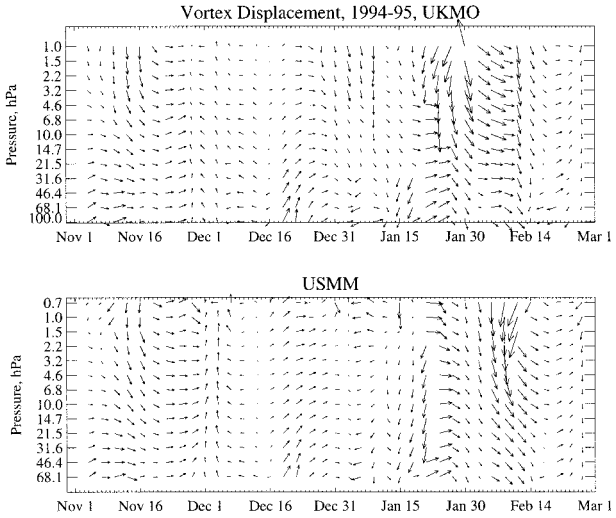

FIG. 22. Vortex displacement diagnostic (as in Fig. 9) for 1994–95.

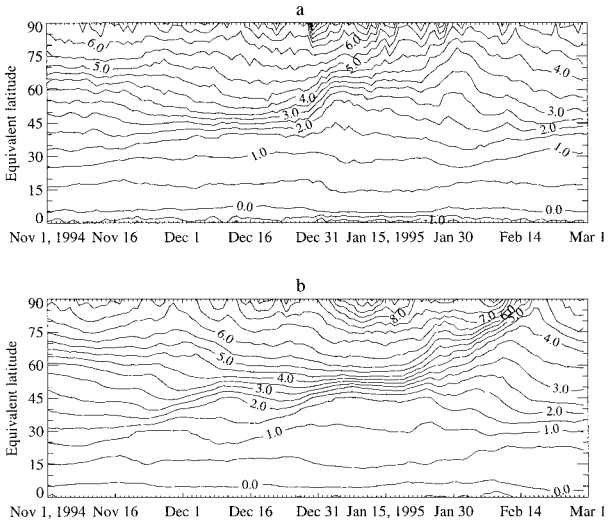

FIG. 23. Potential vorticity area diagnostic at 1400 K (as in Fig. 10) for 1994–95.

after the warming. The large values of F_z in January 1992 appear to be associated with wave 1, while in January 1995 they appear to be associated with wave 2. Wave 3, which had a smaller peak in January 1995 than in January 1992, appears to have played a role in the 1995 warming.

Second, wave warmings are rarely easy to tie to events at the tropopause, while wave 2 warmings are usually deep structures definitely anchored to tropospheric events (A. O'Neill 1997, personal communication). The January 1992 warming, with its wave 1 dominance, may have had less connection to the lower boundary forcing. The subtlety of wave 1 behavior is evident in Fig. 24; both the UKMO and the USMM show examples of apparent downward propagation.

Third, the 1991–92 winter saw several traveling anticyclones, which were generally simulated badly in the USMM. If the traveling anticyclones played a significant role in eroding the vortex that year, as it seems they did, the USMM's failure to produce a warming in January 1992 may be due to the way the USMM simulates traveling anticyclones. The speed and characteristics of traveling anticyclones are not determined directly by the lower-boundary forcing (see Manney et al. 1991) but are determined internally. It is possible that the problem of the traveling anticyclones is related to the poorer simulation of wavenumber 2 in 1991–92 (Fig. 20).

Finally, although the distributions of $\overline{u}$ and $\overline{T}$ look reasonable in the UKMO data on 1 November 1991, they were produced using the same assimilation algorithm that led to the catastrophe in early December. We cannot, without further simulations, rule out the possibility that the seeds of the model's failure were sown in subtly flawed initial conditions.

As many others have pointed out, the stratosphere does not respond simply and linearly to the troposphere. In the first place, events [like the stratospheric warmings in the GCM study of Erlebach et al. (1996), and the wave growth we showed in section 7] often develop downward; and **F** vectors sometimes indicate downward propagation of planetary-scale waves, especially after a warming [see Figs. 5d and 16d, and Randel et al. (1987)]. In the second place, sudden warmings have been known to occur in mechanistic models with *steady* lower-boundary forcing (e.g., Hsu 1981), provided the lower-boundary forcing is of sufficient amplitude. In such situations, the nonlinear dynamics place limits on the success of a mechanistic model simulation that is forced at the lower boundary.

b. Application of the model

In some ways, it is remarkable that a mechanistic model can track observations at all. Its only connection to the observed troposphere is through daily values of 100 hPa heights at resolved scales. Subgrid-scale momentum forcing is treated crudely with a global mean source and an outdated treatment of gravity wave propagation and breaking. (This scheme is, however, a significant advance on the Rayleigh friction used in most mechanistic models.) Temporal and zonal variations in tropospheric temperature and cloudiness, which have a large influence on the infrared radiation reaching the stratosphere, are parameterized using a simplified radiative calculation based on zonally and seasonally varying temperatures at four tropospheric levels. Given these limitations, we consider the model's performance a modest success.

There is, however, room for improvement. The treatment of the infrared flux at the lower boundary has improved considerably since the USMM was developed, when it was a single globally averaged value for the two wavelengths. The improvements already imple-

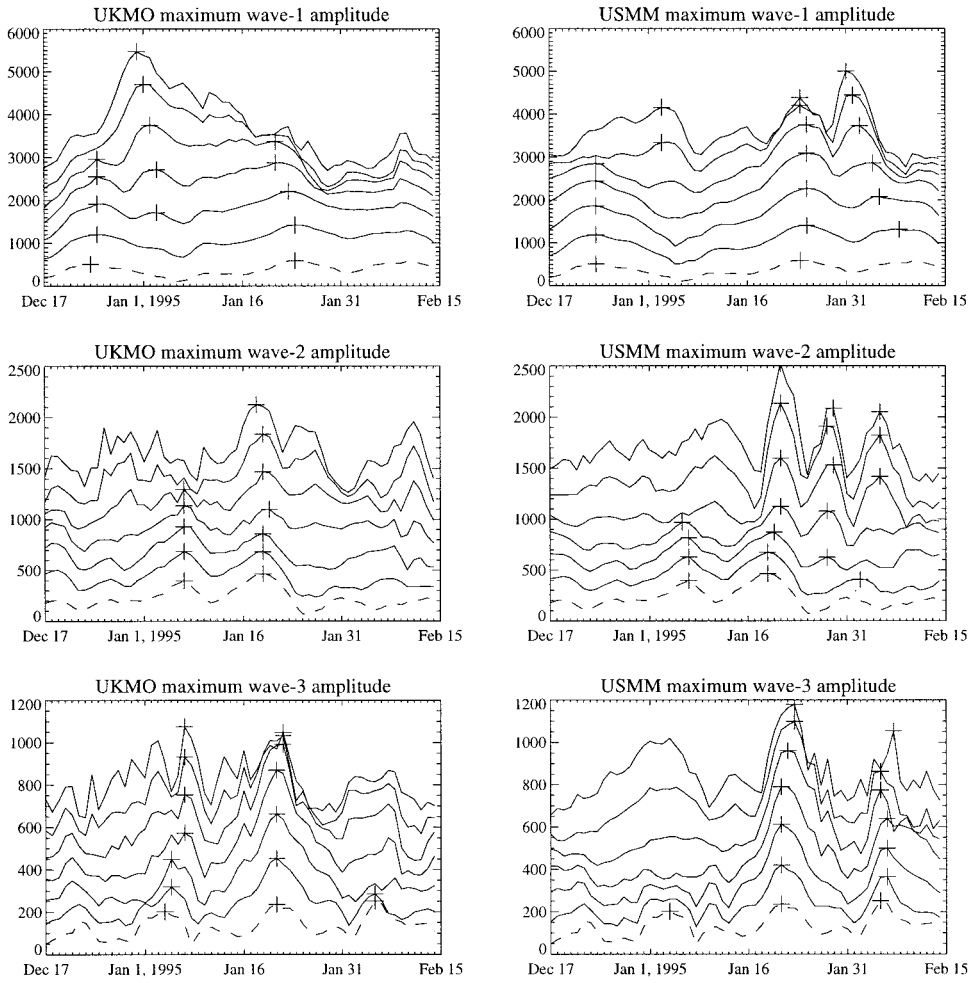

FIG. 24. Hemispheric maximum amplitude of three lowest wavenumbers *m* with curves offset by 400/*m* meters; from top to bottom in each plot, curves represent amplitude at 1.0, 2.2, 4.6, 10.0, 21.5, and 46.4 hPa. UKMO 100-hPa amplitude is shown for both UKMO (left column) and USMM (right column) as the dashed curve. The "+" symbols indicate selected local maxima at each level.

mented have led not just to better temperatures in the lower stratosphere, but to differences in the behavior of the vortex on a given day. It is possible that the model's difficulty in simulating anticyclones would be alleviated by introducing a zonally varying lower boundary IR flux; this could be tested. Another potential change is in the gravity wave scheme; more recent schemes may provide better results, though the gravity wave source at 100 hPa is still poorly known.

The USMM could be (and is) put to use in a number of ways. The experiments performed by Farrara et al. (1992) on the Southern Hemisphere and by Smith (1992) on the Northern Hemisphere suggest some experiments that could, for example, unravel the sequence of events and the importance of various waves in the January 1992 warming, and in particular why the vortex never regained strength in the lower stratosphere (compare Figs. 3 and 13). Another application is in modeling the chemistry of the atmosphere. The USMM has been coupled to a sophisticated chemistry model to investigate a variety of issues surrounding ozone depletion (Stott et al. 1997). In this regard, if one wanted to simulate events day-by-day, high-latitude temperature errors on certain days in the USMM could be serious (Figs. 4 and 14) owing to the temperature dependence of certain chemical reactions and especially of the formation of polar stratospheric cloud particles. On the other hand, in the mean the USMM produces conditions fairly similar to the observed (Figs. 1 and 11), and as Manney et al. (1996b) and Knudsen (1996) have pointed out, UKMO data have a warm bias under conditions when PSCs might form, so the USMM might be doing better than would at first appear.

A final application of the USMM that we mention here is the study of stratospheric predictability. In previous simulations of sudden warmings (e.g., Miyakoda

et al. 1970; Butchart et al. 1982; Simmons and Strüfing 1983; Farrara et al. 1992), models were initialized a few days to a few weeks before the warming in question, and in most cases reproduced the observed structure reasonably well. Note, however, from Fig. 22 that the displacement of the vortex from the pole is reasonably well simulated for the first several weeks of the simulation. It is possible that even after a few weeks the stratosphere has some memory of its initial state, and that we see in Fig. 22 an indication of the predictability of the stratosphere. Predictability will be the subject of a forthcoming paper (Mote and Buizza 1997, unpublished manuscript).

Acknowledgments. We thank John Thuburn, Roger Brugge, and Dave Knowles for developing the USMM; Paul Berrisford and Dingmin Li for supplying the ECMWF data; Gordon Watson and Anne Pardaens for technical assistance; and Hugh Pumphrey for providing maps of PV from the UKMO data. Karen Rosenlof supplied the code to calculate EP fluxes. John Thuburn, William Lahoz, Richard Swinbank, Donal O'Sullivan, and Alan O'Neill gave valuable suggestions; Gloria Manney provided a thorough and constructive review. This work was supported largely by the Natural Environment Research Council (United Kingdom) through UGAMP, and also by the National Aeronautics and Space Administration contracts NAS1-96071 and NAS5-32862. Publication costs were met by NorthWest Research Associates from its internal budget.

REFERENCES

Andrews, D. G., J. R. Holton, and C. B. Leovy, 1987: *Middle Atmosphere Dynamics.* Academic Press, 489 pp.

Beck, A., 1996: The stability of the northern stratospheric winter polar vortex in dependence on the horizontal resolution in a global model. *Beitr. Phys. Atmos.,* **69,** 449–460.

Boville, B. A., 1995: Middle atmosphere version of CCM2 (MACCM2): Annual cycle and interannual variability. *J. Geophys. Res.,* **100,** 9017–9039.

Butchart, N., and E. E. Remsberg, 1986: The area of the stratospheric polar vortex as a diagnostic for tracer transport on an isentropic surface. *J. Atmos. Sci.,* **43,** 1319–1339.

——, S. A. Clough, T. N. Palmer, and P. J. Trevelyan, 1982: Simulations of an observed stratospheric warming with quasigeostrophic refractive index as a model diagnostic. *Quart. J. Roy. Meteor. Soc.,* **108,** 475–502.

Dunkerton, T. J., C. P. F. Hsu, and M. E. McIntyre, 1981: Some Eulerian and Lagrangian diagnostics for a model stratospheric warming. *J. Atmos. Sci.,* **38,** 819–843.

Edmon, H. J., B. J. Hoskins, and M. E. McIntyre, 1980: Eliassen–Palm cross sections for the troposphere. *J. Atmos. Sci.,* **37,** 2600–2616.

Erlebach, P., U. Langematz, and S. Pawson, 1996: Simulations of stratospheric sudden warming in the Berlin troposphere–stratosphere-mesosphere GCM. *Ann. Geophys.,* **14,** 443–465.

Farrara, J. D., M. Fisher, C. R. Mechoso, and A. O'Neill, 1992: Planetary-scale disturbances in the southern stratosphere during early winter. *J. Atmos. Sci.,* **49,** 1757–1775.

Fisher, M., A. O'Neill, and R. Sutton, 1993: Rapid descent of mesospheric air into the stratospheric polar vortex. *Geophys. Res. Lett.,* **20,** 1267–1270.

Harwood, R. S., 1975: The temperature structure of the southern hemisphere stratosphere August–October 1971. *Quart. J. Roy. Meteor. Soc.,* **101,** 75–91.

Hsu, C.-P. F., 1981: A numerical study of the role of wave-wave interactions during sudden stratospheric warmings. *J. Atmos. Sci.,* **38,** 189–23.

Knudsen, B. M., 1996: Accuracy of arctic stratospheric temperature analyses and the implications for the prediction of polar stratospheric clouds. *Geophys. Res. Lett.,* **23,** 3747–3750.

Kouker, W., A. Beck, H. Fischer, and K. Petzoldt, 1995: Downward transport in the upper-stratosphere during the minor warming in February 1979. *J. Geophys. Res.,* **100,** 11 069–11 084.

Leovy, C. B., and P. J. Webster, 1976: Stratospheric long waves: Comparison of thermal structure in the northern and southern hemisphere. *J. Atmos. Sci.,* **33,** 1624–1638.

Manney, G. L., J. D. Farrara, and C. R. Mechoso, 1991: The behavior of wave 2 in the Southern Hemisphere stratosphere during winter and spring. *J. Atmos. Sci.,* **48,** 976–998.

——, ——, and ——, 1994: Simulations of the February 1979 stratospheric sudden warming—Model comparisons and 3-dimensional evolution. *Mon. Wea. Rev.,* **122,** 1115–1140.

——, M. L. Santee, L. Froidevaux, J. W. Waters, and R. W. Zurek, 1996a: Polar vortex conditions during the 1995–1996 Arctic winter: Meteorology and MLS ozone. *Geophys. Res. Lett.,* **23,** 3203–3206.

——, R. Swinbank, S. T. Massie, M. E. Gelman, A. J. Miller, R. Nagatani, A. O'Neill, and R. W. Zurek, 1996b: Comparison of U.K. Meteorological Office and U.S. National Meteorological Center stratospheric analyses during northern and southern winter. *J. Geophys. Res.,* **101,** 10 311–10 334

Matsuno, T., 1971: A dynamical model of the stratospheric sudden warming. *J. Atmos. Sci.,* **28,** 1479–1494.

McIntyre, M. E., 1982: How well do we understand the dynamics of stratospheric warmings? *J. Meteor. Soc. Japan,* **60,** 37–65.

Miyakoda, K., R. F. Strickler, and G. D. Hembree, 1970: Numerical simulation of the breakdown of a polar-night vortex in the stratosphere. *J. Atmos. Sci.,* **27,** 139–154.

Naujokat, B., and K. Labitzke, Eds., 1993: Collection of reports on the stratospheric circulation during the winters 1975/75–1991/92. STEP Handbook, July 1993, SCOSTEP, Urbana, IL.

——, and S. Pawson, 1996: The cold stratospheric winters 1994/1995 and 1995/1996. *Geophys. Res. Lett.,* **23,** 3703–3706.

O'Neill, A., and V. D. Pope, 1988: The seasonal evolution of the extra-tropical middle atmosphere. *Quart. J. Roy. Meteor. Soc.,* **114,** 1063–1110.

——, W. L. Grose, V. D. Pope, H. Maclean, and R. Swinbank, 1994: Evolution of the stratosphere during northern winter 1991/92 as diagnosed from U.K. Meteorological Office analyses. *J. Atmos. Sci.,* **51,** 2800–2817.

O'Sullivan, D., and M. H. Hitchman, 1992: Inertial instability and Rossby-wave breaking in a numerical model. *J. Atmos. Sci.,* **49,** 991–1002.

——, and R. E. Young, 1992: Modeling the quasi-biennial oscillation's effect on the winter stratospheric circulation. *J. Atmos. Sci.,* **49,** 2437–2448.

——, and T. J. Dunkerton, 1994: Seasonal development of the extratropical QBO in a numerical model of the middle atmosphere. *J. Atmos. Sci.,* **51,** 3706–3721.

Palmer, T. N., G. J. Shutts, and R. Swinbank, 1986: Alleviation of a systematic westerly bias in general circulation and numerical weather prediction models through an orographic gravity wave parametrization. *Quart. J. Roy. Meteor. Soc.,* **112,** 1001–1040.

Randel, W. J., 1987: A study of planetary waves in the southern winter troposphere and stratosphere. Part I: Wave structure and vertical propagation. *J. Atmos. Sci.,* **44,** 917–935.

——, 1992: Global atmospheric circulation statistics. NCAR Tech. Note NCAR/TN-366+STR. 256 pp.

——, D. E. Stevens, and J. L. Stanford, 1987: A study of planetary waves in the southern winter troposphere and stratosphere. Part II: Life cycles. *J. Atmos. Sci.,* **44,** 936–949.

Rosier, S. M., B. N. Lawrence, D. G. Andrews, and F. W. Taylor, 1994: Dynamical evolution of the northern stratosphere in early winter 1991/92, as observed by the Improved Stratospheric and Mesospheric Sounder. *J. Atmos. Sci.,* **51,** 2783–2799.

Simmons, A. J., and R. Strüfing, 1983: Numerical forecasts of stratospheric warming events using a model with a hybrid vertical coordinate. *Quart. J. Roy. Meteor. Soc.,* **109,** 81–111.

Smith, A. K., 1992: Preconditioning for stratospheric sudden warmings: sensitivity studies with a numerical model. *J. Atmos. Sci.,* **49,** 1003–1019.

Stott, P. A., G. C. Watson, I. A. MacKenzie, and R. S. Harwood, 1997: COSMIC: A new three-dimensional mechanistic model of the middle atmosphere with an interactive chemistry scheme. *Research Activities in Atmospheric and Oceanic Modelling,* A. Staniforth, Ed., CAS/JSC Working Group on Numerical Experimentation Rep. 25, 7.68.

Swinbank, R. S., and A. O'Neill, 1994: A stratosphere–troposphere data assimilation system. *Mon. Wea. Rev.,* **122,** 686–702.

Thuburn, J., 1992: EUGCM version 2.0 and EUGCM version 2.1. UGAMP Internal Rep. 27.

——, and K. P. Shine, 1991: The MIDRAD radiation scheme in the EUGCM. UGAMP Internal Rep. 17.

Ushimaru, S., and H. Tanaka, 1994: The role of planetary-waves in the formation of inter-hemispheric asymmetry in ozone distribution. *J. Meteorol. Soc. Japan,* **72,** 653–670.

Waugh, D. W., 1997: Elliptical diagnostics of stratospheric polar vortices. *Quart. J. Roy. Meteor. Soc.,*. **123,** 1725–1748.

Zurek, R. W., G. L. Manney, A. J. Miller, M. E. Gelman, and R. M. Nagatani, 1996: Interannual variability of the north polar vortex in the lower stratosphere during the UARS mission. *Geophys. Res. Lett.,* **23,** 289–292.